LAWRENCE
LIVERMORE
NATIONAL
LABORATORY

LLNL-JRNL-639257

Multi--model mean nitrogen and sulfur deposition from the Atmospheric Chemistry and Climate Model Intercomparison Project (ACCMIP): evaluation, historical and projected changes.

J. F. Lamarque, F. Dentener, J. McConnell, C. U. Ro, M. Shaw, R. Vet, D. Bergmann, P. Cameron-Smith, R. Doherty, G. Faluvegi, S. J. Ghan, B. Josse, T. H. Lee, I. A. MacKenzie, D. Plummer, D. T. Shindell, D. S. Stevenson, S. Strode , G. Zeng

June 17, 2013

Atmospheric Chemistry and Physics

Disclaimer

Multi-model mean nitrogen and sulfur deposition from the Atmospheric Chemistry and Climate Model Intercomparison Project (ACCMIP): evaluation, historical and projected changes.

Jean-François Lamarque[1], F. Dentener[2], J. McConnell[3], C.-U. Ro[4], M. Shaw[4], R. Vet[4], D. Bergmann[5], P. Cameron-Smith[5], R. Doherty[6], G. Faluvegi[7], S. J. Ghan[8], B. Josse[9], Y. H. Lee[7], I. A. MacKenzie[6], D. Plummer[10], D. T. Shindell[7], D. S. Stevenson[6], S. Strode[11,12] and G. Zeng[13]

[1] NCAR Earth System Laboratory, National Center for Atmospheric Research, Boulder, CO, USA
[2] European Commission, Joint Research Centre, Ispra, Italy
[3] Desert Research Institute, Reno, NV, USA
[4] Environment Canada, Toronto, Ontario, Canada
[5] Lawrence Livermore National Laboratory, Livermore, CA, USA
[6] School of GeoSciences, University of Edinburgh, Edinburgh, UK
[7] NASA Goddard Institute for Space Studies and Columbia Earth Institute, New York, NY, US
[8] Pacific Northwest National Laboratory, Richland, WA, USA
[9] GAME/CNRM, Météo-France, CNRS - Centre National de Recherches Météorologiques, Toulouse, France
[10] Canadian Centre for Climate Modeling and Analysis, Environment Canada, Victoria, British Columbia, Canada
[11] NASA Goddard Space Flight Center, Greenbelt, MD, USA
[12] Universities Space Research Association, Columbia, MD, USA
[13] National Institute of Water and Atmospheric Research, Lauder, New Zealand

Abstract

We present multi-model global datasets of nitrogen and sulfate deposition covering time periods from 1850 to 2100, calculated within the Atmospheric Chemistry and Climate Model Intercomparison Project (ACCMIP). The computed deposition fluxes are compared to surface wet deposition and ice-core measurements. We use a new dataset of wet deposition for 2000-2002 based on critical assessment of the quality of existing regional network data. We show that for present-day (year 2000 ACCMIP time-slice), the ACCMIP results perform similarly to previously published multi-model assessments. The analysis of changes between 1980 and 2000 indicates significant differences between model and measurements over the United States, but less so over Europe. This difference points towards misrepresentation of 1980 NH_3 emissions over North America. Based on ice-core records, the 1850 deposition fluxes agree well with Greenland ice cores but the change between 1850 and 2000 seems to be overestimated in the Northern Hemisphere for both nitrogen and sulfur species. Using the Representative Concentration Pathways to define the projected climate and atmospheric chemistry related emissions and concentrations, we find large regional nitrogen deposition increases in 2100 in Latin America, Africa and parts of Asia under some of the scenarios considered. Increases in South Asia

are especially large, and are seen in all scenarios, with 2100 values more than double 2000 in some scenarios and reaching >1300 mgN/m2/yr averaged over regional to continental scale regions in RCP 2.6 and 8.5, ~30-50% larger than the values in any region currently (2000). Despite known issues, the new ACCMIP deposition dataset provides novel, consistent and evaluated global gridded deposition fields for use in a wide range of climate and ecological studies.

1. Introduction

The global nitrogen cycle is of importance for a number of key-issues, such as ecology and biodiversity (e.g. Phoenix et al., 2006; Bobbink et al., 2010; Butchart et al., 2010), eutrophication and acidification (e. g. Bouwman et al., 2002; Rodhe et al., 2002; Hicks et al., 2008; Fisher et al., 2011), climate change-carbon cycle interactions (e.g. Thornton et al., 2007; Reay et al., 2008; Zaehle et al., 2010), food and energy production (Sutton et al., 2011). Nitrogen emissions also impact human health through particulate matter and ozone formation. Clearly, nitrogen is central to many aspects of life on Earth (Galloway et al., 2008; Fowler et al., 2012).

Dinitrogen (N_2) is the most abundant component in the atmosphere, but is chemically unreactive, only contributing to tropospheric chemistry through lightning and associated NO formation (Franzblau and Popp, 1989). More reactive atmospheric nitrogen components include oxidized NO_y (=NO+NO_2+other minor inorganic components and organic nitrogens), the long-lived greenhouse gas dinitrous oxide (N_2O; 131±10 years, Prather et al., 2012), and reduced nitrogen NH_x (=NH_3+NH_4), as well as organic nitrogen components such as amines (Kanadidou et al. 2012). NO_y and NH_x are collectively identified as reactive Nitrogen (Nr). Anthropogenic emissions of Nr components are estimated (van Aardenne et al., 2001; Lamarque et al 2010) to have increased by a factor of 5 to 10 since 1850. Knowledge on the link between Nr generation by human activities and its subsequent impacts requires an accurate description of large-scale emissions, atmospheric chemistry, transport and removal, all of which occur on relatively fast timescales compared to nitrogen in the other compartments of relevance to the Earth system: terrestrial, coastal zones and open ocean.

Global atmospheric-chemistry transport models are routinely used as a tool to calculate the global dispersion of Nr. Since individual models are prone to specific errors and multi-model means typically outperform individual models (e.g. Reichler and Kim, 2008; Shindell et al., 2012), it has become common to use model ensemble calculations to improve the quality of the calculations. Previous deposition ensemble studies include Lamarque et al. (2005) using 6 models and focusing on NO_y deposition, Dentener et al. (2006) using 23 models and discussing NO_y, NH_x and SO_x deposition under current and 2 future scenarios, and Sanderson et al. (2008) using 15 models and focusing on export of NO_y and subsequent deposition.

The present study uses deposition fields generated by 10 models that participated in the Atmospheric Chemistry and Climate Model Intercomparison Project (ACCMIP; Lamarque et al., 2012). ACCMIP was designed to inform aspects of the forthcoming Intergovernmental Panel on Climate Change Assessment Report #5 regarding the role of long-term changes in atmospheric chemistry on climate and

vice-versa. In this ACCMIP study, simulations were provided for time slices representative of the period around 1850, 1980, 2000, 2050 and 2100 (see section 2), where the future atmospheric chemistry-climate conditions follow the 4 Representative Concentration Pathways (Moss et al., 2010). Because of the importance of sulfur deposition (in association with nitrogen deposition) for the understanding of soil and water acidification (Fisher et al., 2011), we have included an analysis of sulfur deposition to the more traditional nitrogen deposition analysis. The models used in this analysis represent a combination of the current generation of Chemistry-Transport Models and Chemistry-Climate Models, with somewhat refined horizontal and vertical resolution and more detailed descriptions of chemical processes compared to previous studies (namely the results discussed in Dentener et al., 2006 and Sanderson et al., 2008). Rather than representing specific meteorological years - as in previous studies - each model meteorology is rather representative of the decade under consideration (e.g. 1850-1859; or 2000-2009) and hence include the effect of climate change.

This paper is structured as follows. Section 2 gives a short description of the models and the ACCMIP experiments. We also define there the methodology for computing the multi-model mean (MMM). Section 3 describes the measurement datasets used in this paper, from surface sites and from ice cores. In Section 4, we evaluate the multi-model mean for the 2000 period- when extensive measured deposition datasets are available, and which allows us also to make a retrospective analysis of the quality of data in this model dataset compared to the earlier and widely used Photocomp (Dentener et al., 2006) and HTAP (Sanderson et al., 2008; Vet et al., 2013) deposition datasets. In Section 5, a more limited analysis is given for the changes in deposition (and its drivers) since the 1980s and, using ice-cores, for the change between decades centered around 1850 and 2000. The 1980-2000 period is of particular interest since, due to implementation of national and international emission control measures, strong emission reductions have been reported, especially over North America and Europe, with commensurate consequences for deposition. Section 6 describes the overall global structure of total deposition (dry and wet) from 1850 to 2100. A discussion and conclusions follow in Section 7.

2. ACCMIP simulations and multi-model mean

An overview of the Atmospheric Chemistry and Climate Model Intercomparison Project (ACCMIP) simulations and participating models is given in Lamarque et al. (2012). Consequently, we focus here on the aspects relevant to the analysis of nitrogen and sulfate deposition.

ACCMIP provides analysis on the role of atmospheric chemistry changes in the near-term-climate forcing included in the CMIP5 (Climate Model Intercomparison Project Phase 5; Taylor et al., 2012) simulations, including the chemical composition changes associated with the CMIP5 prescribed forcings. The ACCMIP simulations used in the present study (Table 1) consist of time slice experiments (for specific periods spanning 1850 to 2100 with a minimum increment of 10 years) with chemistry diagnostics. Each requested simulation is

labeled as Primary ("P") or Optional ("O"). Although simulations using the Representative Concentration Pathway 6.0 (RCP6.0, Kainuma et al., 2011) emissions were performed, not enough groups provided the necessary fields for a meaningful analysis of nitrogen and sulfur depositions; therefore, this work focuses on the remaining three RCP projections, RCP2.6, RCP4.5 and RCP8.5 (see van Vuuren et al., 2011 and references therein). A primary output of these simulations was nitrogen and sulfate (dry and wet) deposition fields (see Table S1 in Lamarque et al., 2012). As discussed in Lamarque et al. (2012) and Young and al. (2012), even though the anthropogenic and biomass burning emissions were specified to follow Lamarque et al. (2010) for 1850-2000 and the RCP emissions (van Vuuren et al., 2011) beyond, there is a range of emissions that were used in ACCMIP models, mostly from variations in the treatment of natural emissions.

As a first step in the quality control of the model calculated depositions, we analyze for each model the balance between emission and deposition as reported by the modeling groups (Tables 2-4) for the year 2000 time slice experiment. This analysis is done separately for nitrogen originating from nitrogen oxide emissions (deposition fields are referred as a group as NO_y) or ammonia emissions (NH_x) and sulfur emissions (SO_x). We find that the NO_y deposition is larger than the emissions (surface and upper-air, including lightning) by approximately 1 Tg(N)/year, representing the input of nitrogen (mostly in the form of nitric acid) from the stratosphere, in general agreement with observational estimates of 0.45 Tg(N)/year from Murphy and Fahey (1998), except for the GISS model where this influx is approximately 5 Tg(N)/year. In the case of ammonium, the balance between emissions and deposition is clearly attained. In the case of sulfur, this balance cannot be fully evaluated due to the lack of diagnostics on the formation of sulfate aerosols from the emitted dimethylsulfide (DMS). Boucher et al. (2003) estimated the yield (DMS to sulfate aerosols) to be 87% when both gas-phase and aqueous-phase reactions are taken into account, but this number will be somewhat model dependent. Within that limitation, it is reasonable to assume that balance between sulfur deposition and emission is achieved for the listed models.

The focus of this paper is on documenting the multi-model mean (MMM) generated for each time slice. The MMM is constructed by linearly interpolating the model generated monthly fields (for example wet deposition combined for all NO_y species) at their native horizontal resolution (Table S1) to a common 0.5°x0.5° grid (finer than any model grid), identical to the emission grid used in Lamarque et al. (2010). Then, each field is averaged across models at the original monthly temporal resolution to generate its multi-model mean and standard deviation (Table S2-S4). As indicated in these tables, the largest number of models (up to 9) generated the necessary fields is found for the historical NO_y deposition, followed by the RCP8.5 simulations. The number of models performing ammonium chemistry and deposition is however much smaller (2-3 models, depending on the simulated time period) while between 2 and 6 models have provided sulfate fields. In all cases, the MMM is constructed using all available model results, therefore leading to variations between the specific models used in the average.

3. Description of observational deposition data

Under the auspices of the World Meteorological Organization (WMO), a precipitation chemistry expert group has performed a critical analysis of available wet deposition data for the years 2000 to 2002. While dry deposition may be available at specific sites, this is not a directly observed quantity and we therefore do not use this information. We use the WMO-processed wet deposition datasets in our analysis of the performance of the MMM in the 2000 time slice.

In the WMO dataset, a careful analysis is made of worldwide reported data of wet precipitation chemistry, and data quality qualifiers are provided to deposition data obtained mainly from networks in Europe (European Monitoring and Evaluation Programme, EMEP; http://www.nilu.no/projects/ccc/emepdata.html); the United States (National Atmospheric Deposition Program, NADP; http://nadp.sws.uiuc.edu/NTN/ntnData.aspx); Canada (Canadian Air and Precipitation Monitoring Network, CAPMoN; http://www.ec.gc.ca/rs-mn/default.asp?lang=En&n=752CE271-1); Asia (mainly from the Acid Deposition Monitoring Network in East Asia, EANET; http://www.eanet.cc), and Africa (Deposition of Biogeochemically Important Trace Species (DEBITS), http://debits.sedoo.fr). We will focus our analysis on the NADP, EMEP and EANET observations. For more detailed information on data networks, data selection criteria, and an application to the HTAP Phase 1 deposition dataset, we refer to Vet et al. (2013), as well as the data networks indicated above. The evaluated wet deposition datasets, soon to be available through the World Data Centre for Precipitation Chemistry, only contain a subset of the available stations for that period, i.e. stations that correspond to regionally representative sites that fulfilled specific data completeness and quality control measures. In this paper, we use the wet deposition measurements of nitrate (NO_3), ammonium (NH_4) and non-sea salt sulfate (SO_4), which were qualified as 'good'.

Over Europe (EMEP) and the United States (NADP), deposition measurement sites typically started around the 1980s. We use these early measurements to evaluate the change in deposition over these two decades. To this purpose, we computed from the raw data (available at the aforementioned web sites), and using the filtering protocols defined by the specific networks, two sets of 6-year averages (1980-1985 and 1997-2002) for sites that had sufficient observations for both time slices.

Although a quality control similar to the WMO evaluation was not available for the 1980s data, comparison of the WMO processed 2000-2002 data with our 1997-2002 indicate very good agreement over the respective regions (not shown), validating the suitability of our processed dataset to study trends in deposition from the 1980s to the 2000s.

Historical records of nitrate, ammonium, and sulfur were also developed from high-depth-resolution measurements in ice cores (see Table S5 for their geographical information) using an established continuous ice core analytical system (e.g., McConnell and Edwards, 2008). Nitrate and ammonium were measured using spectrophotometry and fluorimetry, respectively, with standard flow through methods (Roethlisberger et al., 2000). Total sulfur concentrations were measured using magnetic sector Inductively Coupled Plasma Mass

Spectrometry (McConnell and Edwards, 2008). At core sites with sufficient annual snowfall, the ice core records were dated using annual layer counting of a range of seasonally varying chemical species (Sigl et al., 2012). Synchronization to well-known volcanic layers was used for dating at core sites with very low snowfall (e.g., East Antarctica) where annual layers are not preserved (Anschütz et al. 2011) or at lower elevation sites (e.g., Akademmi Nauk, McCall Glacier, Flade Isblink) where surface melting and percolation make annual layer identification difficult (Opel et al. 2009). Uncertainty (1 sigma) in the dating is estimated at +/- 1 year for the annually dated sites and +/- 3 years for all other sites. Decadal averages centered on 1855 and 2000 were computed from the high-resolution measurements.

4. Evaluation of ACCMIP year 2000 time slice deposition

While observation and model data are available at the monthly time resolution, we focus our analysis on the annual mean. This choice is made to limit the discussion to the long-term trends in nitrogen and sulfate deposition. In addition to the present intercomparison project, MMM results from two previous studies are available for comparison and analysis of potential improvements: PhotoComp (Dentener et al., 2006) and HTAP (Sanderson et al., 2012; Vet et al., 2013). These previous studies are partially independent of the present one, with different emissions and a different sets of models or different versions of the same models. Using the WMO dataset and the model results interpolated to the location of the observing stations, we can statistically analyze the ability of the models to reproduce the observations.

We display in Figure 1 the global and regional distributions of NO_3 (panel a), NH_4 (panel b) and SO_4 (panel c) wet deposition in the MMM compared to the WMO dataset (over Europe and the United States). Deposition is clearly strongly correlated with emissions (i.e. largest in the Northern Hemisphere, but also with larger amounts in areas of biomass burning and large soil emissions such as Central Africa), albeit with significant downwind propagation for each compound. Unlike the nitrogen sources, sulfur emissions from degassing volcanoes (Andres and Kasgnoc, 1998) lead to the formation of deposition hotspots in areas with low anthropogenic emission levels such as Central America.

In the case of NO_3 deposition, we find that all 3 experiments (ACCMIP, HTAP and PhotoComp) perform rather similarly (Figure 2 and Table 5). However, none of the model simulations are able to capture the observed high deposition rates over East Asia or Europe, possibly due to the close proximity of the observing stations to significant sources, features that cannot easily be captured with the coarse grid of presently used models (Zhang et al., 2012). In contrast, in the high emission region of Northeastern United States, there are regions of overestimation as well as underestimation.

In the case of NH_4, the ACCMIP results are slightly lower than the previous studies over both the North American NADP and European EMEP domains and therefore with a larger negative bias. Owing to NH3 emission regridding issue in the agricultural emissions over China in ACCMIP (see http://www.iiasa.ac.at/web-apps/tnt/RcpDb/dsd?Action=htmlpage&page=download), the performance in

ACCMIP (Figure 2) is considerably worse than the previous studies over Asia, with a significant underestimate (by approximately 30%, see Table 5) for the highest deposition rates over East Asia.

The sulfate deposition is somewhat improved in ACCMIP over the NADP stations, while the very high biases previously found in the HTAP dataset over the EMEP domain are now considerably reduced, so that the ACCMIP models might actually be underestimating wet deposition over that region. The deposition over EANET is characterized by a larger negative bias in ACCMIP than PhotoComp or HTAP, although the overall correlation remains high.

Overall, the performance of the ACCMIP MMM is similar to PhotoComp and HTAP, suggesting that no significant improvement or worsening has been made since those 2 studies in the representation of emissions, chemical processing and deposition processes. The analysis also shows that ammonium deposition over East Asia is most likely underestimated. On the other hand, for all considered species, the ACCMIP MMM deposition tends to be slightly overestimated over the NADP stations.

5. Evaluation of historical deposition changes: 1980-2000 and 1850-2000

To identify potential changes in deposition over time, we use the 1980 and 2000 time slice experiments. Unfortunately, neither HTAP nor PhotoComp provide historical time slices and therefore such changes cannot be discussed within that context. Over that period, Europe and North America have seen significant changes in nitrogen and sulfur emissions, from a combination of changes in anthropogenic activities and air quality regulations (Granier et al., 2011; Xing et al., 2012).

To limit issues associated with interannual variability and uneven time sampling from the observed wet deposition rates, we require that each station much have at least 36 months of available data for each 6-year averaging period (see section 3).

Over the United States, the NADP measured nitrate deposition change between 1980 and 2000 consists mostly of reductions, especially in the eastern portion of the United States (Fig. 3a). However, the MMM shows only a minor change over the western United States, and actually simulates a minor increase over the eastern States. Indeed, all models except GISS (Table 6) indicate a relative increase in nitrate deposition averaged over the United States. This simulated increase in wet deposition is a combination of minor increases in NO_x emissions (Fig. S1a) and in precipitation amounts (Table 6). Based on the CPC Merged Analysis of Precipitation (CMAP; Xie and Arkin, 1997), there is however indication of a small observed decrease in precipitation between 1980 and 2000 over the United States (Figure S2), while the MMM has limited inter-model agreement and actually shows a slight increase in precipitation when averaged over the whole United States (Table 6). It must however be recognized that the changes over the United States are relatively small and may therefore be strongly affected by interannual variability. Over the EMEP network, many sites indicate a very strong reduction consistent with emission change (Fig. S1a), with the exception of former Yugoslavia and the southern tip of Norway. The MMM captures well the strong

reduction, with however a smaller amplitude than is observed at most locations. In this case (Table 6), all models agree on the change in emissions (-12% for the mean) and all but MOCAGE show an increase in precipitation.

Measured ammonium deposition (Fig. 3b) changes over the NADP network show a mixture of increases and decreases, with again the largest decreases over the Northeastern United States. Similar to nitrate deposition, the MMM is much more uniform than observed and only shows a small decrease in the mid-Western United States. This is due to the fact that the anthropogenic emissions of NH_3 are almost identical between 1980 and 2000 (see Figure S1b). This is possibly erroneous but more analysis is beyond the scope of this paper. Over Europe, the EMEP station data indicate an overall strong decrease, with the exception of sites in France, Italy and Norway. In contrast, the MMM indicates an overall small increase over Western Europe and a decrease over Eastern Europe, consistent with the significant emission change (Fig. S1b). Local factors, not included in the models, play a role in these differences.

Over the United States, except for a dozen sites scattered over the NADP network, observed sulfate deposition east of 100°W (Fig. 3c) is characterized by large reductions driven by emission change (Fig. S1c). The MMM is however underestimating the amplitude of the changes, especially for the largest changes. Over the EMEP network, the MMM captures well the general deposition decrease including its largest change over Germany, clearly in agreement with the emission change (Fig. S1c).

Overall, the analysis of changes between 1980 and 2000 shows limited agreement between MMM and observations over the United States. In particular, the observed changes over the NADP network indicate much higher variability and amplitude than is simulated, driven by fairly small changes in emissions. Also, this analysis highlights the potential error in the NH_3 emission change over the United States between 1980 and 2000. While the deposition change over Europe from the MMM is not as large as observed, the overall patterns of change are much better represented, except for NH_x deposition over Western Europe. This suggests that NO_x (and to a lesser extent SO_x and NH_x) emissions changes may better captured over Europe in the historical emission dataset used in ACCMIP (Lamarque et al., 2010), since emission change is the main driver for deposition change. However, further analysis is required for a complete understanding of the applicability of deposition data to constrain emission inventories.

In addition, we use ice core records of deposition over the Northern hemisphere and over Antarctica to study the ability of the models to represent changes since 1850. To limit the importance of interannual variability in the ice-core record, we use the average values for 1850-1860 and 1995-2005 to compare against the 1850 and 2000 time slices, respectively. As a basic test of the applicability of the MMM to the polar regions, we show in Figure S3 a comparison of year 2000 precipitation against the gauge-based climatology of Yang et al. (2005). We find that the MMM compares rather well to the observations throughout the Arctic circle, with the caveat that no rain gauge is available over Central Greenland. Additional analysis of precipitation over the Arctic is provided in Lee et al. (2012). No equivalent data are available for Antarctica.

We find that there is a strong agreement between the 1850 observed and simulated nitrate depositions (Fig. 4a) for 1850, both in regional structure and intensity. Nitrate deposition in 2000 is however overestimated at all Northern hemisphere sites but one. On the other hand, the year 2000 simulated deposition over Antarctica, which is much less affected by changes in anthropogenic NO_x emissions but still shows an overall increase in nitrate deposition, is in good agreement with the observations.

Ammonium deposition (Fig. 4b) is strongly overestimated at the Greenland sites in both 1850 and 2000 time slices (and so is the change 2000 *minus* 1850; not shown). Wolff et al. (2013) argue that it is actually difficult to derive a change of measured NH_4 deposition over Greenland, due to the large dependency on the highly variable contribution of biomass burning to NH_4 deposition. On the other hand the other two sites in the Northern hemisphere (McCall, Alaska and Akademmi Nauk, Siberia; see Table S5 for their exact locations) are well captured. This is true for the 2000 time slice as well, where the McCall glacier shows a decrease since 1850, possibly associated with a change in biomass burning emissions over North America. Over Antarctica, ammonium deposition rates over the Western portion of the ice shelf are well represented, while they are somewhat overestimated in the eastern sector. This is the case for both 1850 and 2000. Increases in the simulated deposition between 1850 and 2000 seem to be larger than observed, albeit the levels of deposition are small compared to those observed in the Northern Hemisphere.

Sulfate deposition in 1850 (Fig. 4c) is represented quite well at the Northern Hemisphere and Antarctic sites, except for McCall, Alaska and central Greenland (Tunu glacier). Sulfate deposition in 2000 is overestimated at all ice-core sites of the Northern Hemisphere. Sulfate deposition over Antarctica has a well-defined east-west separation, well captured by the model. There is little variation between 1850 and 2000 since the sulfate production is primarily driven by DMS oxidation. In many models used in ACCMIP, the DMS source does not vary with time, although Cameron-Smith et al. (2011) suggest it should, and changes in DMS emissions could represent an important feedback in the climate system (Charlson et al, 1987).

Overall, the ice-core comparison of the MMM indicates a reasonable representation of the pre-industrial (1850) conditions but tends to overestimate the present-day (2000) conditions. Similar conclusions are found for 1980 (not shown), indicating that biases in the year 2000 deposition fields are not related to transient features in ice formation.

6. Total nitrogen and sulfate deposition

In this section, we document the MMM global and regional distributions of total deposition (wet + dry) of NO_y, NH_x and SO_x and their changes from 1850 to 2100 under the RCP2.6, 4.5 and 8.5 projection scenarios (Fig. 5 and Tables S2-S4).

The historical increase of NO_y deposition (Fig. 5a) since 1850 took place mostly in the Northern Hemisphere. It is characterized by deposition rates larger than 1 kg(N)/ha/year over most of the continental areas, the North Atlantic and the outflow oceanic areas of Eastern Asia, the Indian subcontinent and Central Africa.

By 2030, the projections over the United States and Europe are quite similar for RCP2.6 and RCP4.5, while RCP8.5 shows a smaller reduction from the 2000 levels. In Eastern Asia, deposition of NO_y is showing levels above 2000, with the largest increase seen in RCP8.5. On the other hand, over the Indian sub-continent, the largest deposition increases were found in RCP4.5. Only small changes occur in the Southern Hemisphere. By 2100, most of the continental areas, except for India, are projected to return to pre-1980 levels of deposition. Another exception is the larger deposition over the Northern Pacific ocean in RCP8.5, consistent with NO_x emissions from shipping. Since the MMM NOy deposition is computed from the largest number of models, it is reasonable to document intermodel variability for that diagnostic (Fig. S6). We find that over most continental areas and for most time slices, the inter-model standard deviation is in the 10-20 % range, with Central Asia and South America being somewhat larger (20-30%).

While the increases in nitrogen deposition from ammonia emissions between 1850 and 2000 affect the various regions similarly to the impact of NO_x emissions (Fig. 5b), the RCP projections for NH_3 emissions are indicative of a very different trajectory (Lamarque et al., 2011), with continuous increases over most continental and oceanic regions, with the exception of the oceans south of 30°S. These deposition changes are mainly driven by the projected increases in inorganic fertilizer use needed to provide more and higher quality food for a growing worldwide population, with no policies in places to abate the emissions.

Simulated sulfate deposition reached higher levels and was more widespread in Europe than North America in 1980, but was similar in both regions by 2000. The only significant increase between 1980 and 2000 is over China, associated with its increasing use of coal for power generation (Smith et al., 2011). The projected changes over these regions indicate a gradual phase-out of anthropogenic emissions by 2100, including over China. Even by 2030, emissions over China are projected to be no larger than in 2000, a trend that might be reflected in the most recent estimates over China (Smith et al., 2011; Klimont et al., 2013). Similar to NO_y deposition, only the Indian subcontinent is projected in RCP8.5 to have sulfate deposition levels higher in 2100 than in 1980. Sulfate deposition over the oceans is also considerably reduced in the RCP scenarios, but depends on the specific scenarios for their projection of shipping emissions.

The combination of deposition fluxes as $2*SO_x+NO_y-NH_x$ provides an indication of the degree of acidity (Fisher et al., 2011) contained in the deposited fluxes (Figure 6). In particular, it clearly shows that, over the 21st century, continental areas over the Northern Hemisphere will have a tendency towards more basic deposition with the increase NH_3 emissions. This analysis also clearly shows the spurious NH3 emissions over Mongolia (as discussed in Section 4).

Following the discussion of averaged deposition rates over various regions in Lamarque et al. (2011, see their Tables 5 and 6; note that the NCAR-CAM3.5 results used in the present ACCMIP analysis are equivalent to results in those), we present the same diagnostics here (in the same units), with the exception of RCP6.0 (Table 7 and 8). Overall, the total (from NO_y and NH_x combined, since both affect vegetation in the same fashion) nitrogen deposition is expected to increase between 2000 and 2100 over many regions, especially in the case of RCP8.5. Furthermore, only Europe

and North America are projected to see a reduction in their nitrogen deposition. Sulfate deposition rates are clearly projected to significantly decrease by 2100, as expected from Fig. 5. All these confirm the results published in Lamarque et al. (2011) in a single model study using the same emission fields applied in the present study.

7. Discussion and conclusions

We have presented in this paper the multi-model mean annual deposition of nitrogen and sulfate as simulated in the Atmospheric Chemistry and Climate Model Intercomparison Project (Lamarque et al., 2012). We have made considerable use of network-based wet deposition datasets (including a new dataset based on expert analysis of the deposition data; Vet et al., 2013) and ice-core records to evaluate deposition rates and changes in the deposition since 1980 and 1850. We have found that the ACCMIP multi-model mean behaves rather similarly to previous multi-model analysis (Dentener et al., 2006; Sanderson et al., 2008), with the notable exception of ammonium deposition over Asia, which is considerably worse in ACCMIP due a re-gridding error in the underlying emissions over that region (Lamarque et al., 2010).

Beyond the present-day analysis, we discuss a comparison of the change in deposition rates between 1980 and 2000 (using surface wet deposition) and between 1850 and 2000 (using ice-cores). Although the deposition in 2000 is rather well simulated in ACCMIP, there are considerable differences between the estimated change from 1980 to 2000 and the simulated one. This is particularly the case over the United States, where changes in anthropogenic NH_x (and to a lesser extent NO_x) emissions are much smaller than over Europe, and do not lead to the observed deposition rate changes. In terms of ice-core analysis, the ACCMIP multi-model mean captures many of the regional features of deposition, but there seems to be an overall estimation in 2000, in the Northern Hemisphere Arctic, while Antarctic deposition fluxes are well represented.

The discussion of the total deposition (wet + dry) in the ACCMIP multi-model mean confirms to a large qualitative extent the single-model results discussed in Lamarque et al. (2011). In particular, there are large regional increases in 2100 N deposition in Latin America, Africa and parts of Asia under some of the scenarios considered. Increases in South Asia are especially large, and are seen in all scenarios, with 2100 values more than double 2000 in some scenarios and reaching region averaged values of >1300 mgN/m2/yr in RCP 2.6 and 8.5 , ~30-50% larger than the values in any region currently (2000). The multi-model mean deposition fields as discussed in this study are available as http://acd.ucar.edu/~lamar/ACCMIP/Deposition/all_fields.tar.gz.

The analysis presented here shows that there is strong potential in using nitrogen and sulfate deposition observational data to identify gaps in our understanding of the respective precursor emissions. Expansion of the WMO wet deposition assessment and more ice cores will provide a window on nitrogen and sulfate emissions, possibly helping to understand difficulties for models to

reproduce long-term trends such as surface ozone in the Northern Hemisphere (Lamarque et al., 2010).

Acknowledgments

ACCMIP is organized under the auspices of Atmospheric Chemistry and Climate AC&C, a project of International Global Atmospheric Chemistry (IGAC) and Stratospheric Processes And their Role in Climate (SPARC) under the International Geosphere-Biosphere Project (IGBP) and World Climate Research Program (WCRP). The authors are grateful to the British Atmospheric Data Centre (BADC), which is part of the NERC National Centre for Atmospheric Science (NCAS), for collecting and archiving the ACCMIP data. D. S., G. F. and Y. L. acknowledge support from the NASA MAP and ACMAP programs. D. P. would like to thank the Canadian Foundation for Climate and Atmospheric Sciences for their long-running support of CMAM development. S. G. was supported by the US Department of Energy Office of Science Decadal and Regional Climate Prediction using Earth System Models (EaSM) program. The Pacific Northwest National Laboratory (PNNL) is operated for the DOE by Battelle Memorial Institute under contract DE-AC06-76RLO 1830. The work of D. B. and P. C.-S. was funded by the US Dept. of Energy (BER), performed under the auspices of LLNL under Contract DE-AC52-07NA27344, and used the supercomputing resources of NERSC under contract No. DE-AC02-05CH11231. G. Z. acknowledges NIWA HPCF facility and funding from New Zealand Ministry of Science and Innovation. The GEOSCCM work was supported by the NASA Modeling, Analysis and Prediction program, with computing resources provided by NASA's High-End Computing Program through the NASA Advanced Supercomputing Division. The STOC-HadAM3 work was supported by cross UK research council grant NE/I008063/1 and used facilities provided by the UK's national high-performance computing service, HECToR, through Computational Modelling Services (CMS), part of the NERC National Centre for Atmospheric Science (NCAS). The MOCAGE simulations were supported by Météo-France and CNRS. Supercomputing time was provided by Météo-France/DSI supercomputing center. The CESM project (which includes CESM-CAM-Superfast, NCAR-CAM3.5 and NCAR-CAM5.1) is supported by the National Science Foundation and the Office of Science (BER) of the US Department of Energy. The National Center for Atmospheric Research is operated by the University Corporation for Atmospheric Research under sponsorship of the National Science Foundation. CMAP Precipitation data are provided by the NOAA/OAR/ESRL PSD, Boulder, Colorado, USA, from their Web site at http://www.esrl.noaa.gov/psd/. We thank Robert Vet and his precipitation chemistry assessment team, to make the WMO deposition dataset available prior to publication.

References

Andres, R. J. and Kasgnoc, A. D. A time-averaged inventory of subaerial volcanic sulfur emissions, *J. Geophys. Res*., 103, D19, 25251–25261, doi:10.1029/98JD02091, 1998.

Anschütz, H., Sinisalo, A., Isaksson, E., McConnell, J. R., Hamran, S.-E., Bisiaux, M. M., Pasteris, D., Neumann, T. A., and Winther, J.-G.. Variation of accumulation rates over the last eight centuries on the East Antarctic Plateau derived from volcanic signals in ice cores*, J. Geophys. Res*., 116, D20103, doi:10.1029/2011JD015753, 2011.

Boucher, O., Moulin, C., Belviso, S., Aumont, O., Bopp, L., Cosme, E., von Kuhlmann, R., Lawrence, M. G., Pham, M., Reddy, M. S., Sciare, J., and Venkataraman, C.: DMS atmospheric concentrations and sulphate aerosol indirect radiative forcing: a sensitivity study to the DMS source representation and oxidation, *Atmos. Chem. Phys*., 3, 49-65, doi:10.5194/acp-3-49-2003, 2003.

Bobbink, R., Hicks, K., Galloway, J., Spranger, T., Alkemade, R., Ashmore, M., Bustamante, M., Cinderby, S., Davidson, E., Dentener, F., Emmett, B., Erisman, J.W., Fenn, M., Gilliam, F., Nordin, A., Pardo, L. and de Vries, W. Nitrogen deposition and plant diversity, *Ecological Applications*, 20 (1), 30-59, 2010.

Bouwman, A. F., Van Vuuren, D. P., Derwent, R. G. and Posch, M. A global analysis of acidification and eutrophication of terrestrial ecosystems, *Water Air Soil Pollut*., 141, 349– 382, doi:10.1023/A:1021398008726, 2002.

Butchart, S. H. M., Walpole, M., Collen, B., van Strien, A., Scharlemann, J.P. W., Almond, R. E. A., Baillie, J. E. M., Bomhard, B., Brown, C., Bruno, J., Carpenter, K. E., Carr, G. M., Chanson, J., Chenery, A.M., Csirke, J., Davidson, N. C., Dentener**,** F., Foster, M., Galli, A., Galloway, J. N., Genovesi, P., Gregory, R. D., Hockings, M., Kapos, V., Lamarque, J.-F., Leverington, F., Loh, J., McGeoch, M. A., McRae, L., Minasyan, A., Hernández Morcillo, M., Oldfield, T. E. E., Pauly, D., Quader, S., Revenga, C., Sauer, J. R., Skolnik, B., Spear, D., Stanwell-Smith, D., Stuart, S. N., Symes, A., Tierney, M., Tyrrell, T. D., Vié, J. and Watson, R. Global Biodiversity: Indicators of Recent Declines, doi:10.1126/science.1187512, *Science,* 328, 1164, 2010.

Cameron**-**Smith, P., Elliott, S., Maltrud, M., Erickson, D. and Wingenter, O. Changes in dimethyl sulfide oceanic distribution due to climate change, *Geophys. Res. Lett*., 38, L07704, doi:10.1029/2011GL047069, 2011.

Charlson, R.J., Lovelock, J.E., Andreae, M.O., Warren, S.G, Oceanic phytoplankton, atmospheric sulphur, cloud albedo, and climate, Nature, 326, 1987.

Dentener, F., Drevet, J., Lamarque, J. F., Bey, I., Eickhout, B.,Fiore, A. M., Hauglustaine,D., Horowitz, L. W., Krol, M., Kulshrestha,U. C., Lawrence, M., Galy-Lacaux, C., Rast, S., Shindell,D., Stevenson, D., Van Noije, T., Atherton, C., Bell, N.,

Bergman, D., Butler, T., Cofala, J., Collins, B., Doherty, R., Ellingsen, K., Galloway, J., Gauss, M., Montanaro, V., Muller,J. F., Pitari, G., Rodriguez, J., Sanderson, M., Solmon, F., Strahan,S., Schultz, M., Sudo, K., Szopa, S., and Wild, O.: Nitrogenand sulfur deposition on regional and global scales: Amultimodel evaluation, *Global Biogeochem. Cy*., 20, GB4003,doi:10.1029/2005GB002672, 2006.

Fisher, J.A., Jacob, D.J., Wang, Q., Bahreini, R., Carouge, C.C., Cubison, M.J., Dibb, J.E., Diehl, T., Jimenez, J.L., Leibensperger, E.M., Lu, Z., Meinders, M.B.J., Pye, H.O.T., Quinn, P.K., Sharma, S., Streets, D.G., van Donkelaar, A. and Yantosca, R.M. Sources, distribution, and acidity of sulfate-ammonium aerosol in the Arctic in winter-spring, *Atmos. Environ*., 45, 7301-7318, 2011.

Fowler, D., Coyle, M., Skiba, U., Sutton, M., Cape, N., Reiss, S., Sheppard, L., Jenkins, A., Galloway, J., Vitousek, P., Leech, A., Bouwman, L., Butterbach-Bahl, K., Dentener, F. Stevenson, D. Amann M., and Voss, M. The Global Nitrogen Cycle in the 21st century, submitted to *Philosophical Transactions of the Royal Society, Series B*, 2012.

Franzblau, E. and Popp, C. J. Nitrogen oxides produced from lightning, *J. Geophys. Res*., 94, D8, 11089–11104, doi:10.1029/JD094iD08p11089, 1989.

Galloway, J. N., Townsend, A. R., Erisman, J. W., Bekund, M., Cai, Z., Freney, J. R., Martinelli, L. A., Seitzinger, S. P., and Sutton, M. A.: Transformation of the nitrogen cycle: recent trends, questions and potential solutions. *Science*, **320**, 889-889, 2008.

Granier, C., Bessagnet, B., Bond, T., D'Angiola, A., Denier van der Gon, H., Frost, G., Heil, A., Kaiser, J., Kinne, S., Klimont, Z., Kloster, S., Lamarque, J.-F., Liousse, C., Masui, T., Meleux, F., Mieville, A., Ohara, T., Raut, J.-C., Riahi, K., Schultz, M., Smith, S., Thompson, A., van Aardenne, J., van der Werf, G., and van Vuuren, D.: Evolution of anthropogenic and biomass burning emissions of air pollutants at global and regional scales during the 1980–2010 period, Climatic Change, 109, 163–190, 2011.

Kanakidou, M., R.A. Duce, J.M. Prospero, A.R. Baker, C. Benitez-Nelson, F.J. Dentener, K.A. Hunter, P.S. Liss, N. Mahowald, G.S. Okin, M. Sarin, K. Tsigaridis, M. Uematsu, L.M. Zamora, and T. Zhu, 2012: Atmospheric fluxes of organic N and P to the global ocean. *Global Biogeochem. Cycles*, **26**, GB3026, doi:10.1029/2011GB004277.

Klimont, Z., Smith, S. J. and Cofala, J. The last decade of global anthropogenic sulfur dioxide: 2000–2011 emissions. *Environ. Res. Lett.,* 8**,** 014003, doi:10.1088/1748-9326/8/1/014003, 2013.

Lamarque, J. F., Kiehl, J. T., Brasseur, G. P., Butler, T., Cameron-Smith, P., Collins, W. D., Collins, W. J., Granier, C., Hauglustaine,D., Hess, P. G., Holland, E. A., Horowitz, L., Lawrence,M. G., McKenna, D., Merilees, P., Prather, M. J., Rasch, P. J.,Rotman, D., Shindell, D., and Thornton, P.: Assessing future nitrogen deposition and carbon cycle

feedback using a multimodel approach: Analysis of nitrogen deposition, *J. Geophys. Res*., 110, D19303, doi:10.1029/2005JD005825, 2005.

Lamarque, J.-F., Bond, T. C., Eyring, V., Granier, C., Heil, A., Klimont, Z., Lee, D., Liousse, C., Mieville, A., Owen, B., Schultz, M. G., Shindell, D., Smith, S. J., Stehfest, E., Van Aardenne, J., Cooper, O. R., Kainuma, M., Mahowald, N., McConnell, J. R., Naik, V., Riahi, K., and van Vuuren, D. P.: Historical (1850–2000) gridded anthropogenic and biomass burning emissions of reactive gases and aerosols: methodology and application, *Atmos. Chem. Phys*., 10, 7017-7039, doi:10.5194/acp-10-7017-2010, 2010.

Lamarque, J.-F., G. P. Kyle, M. Meinshausen. K. Riahi, S. J. Smith, D. P. van Vuuren, A. Conley, F. Vitt. Global and regional evolution of short-lived radiatively-active gases and aerosols in the Representative Concentration Pathways.
Lamarque, J.-F., Kyle, G. P., Meinshausen, M., Riahi, K., Smith, S. J., van Vuuren, D. P., Conley, A., and Vitt, F.: Global and regional evolution of short-lived radiatively-active gases and aerosols in the Representative Concentration Pathways, *Climatic Change*, doi:10.1007/s10584-011-0155-0, 2011.

Lamarque, J.-F., Shindell, D. T., Josse, B., Young, P. J., Cionni, I., Eyring, V., Bergmann, D., Cameron-Smith, P., Collins, W. J., Doherty, R., Dalsoren, S., Faluvegi, G., Folberth, G., Ghan, S. J., Horowitz, L. W., Lee, Y. H., MacKenzie, I. A., Nagashima, T., Naik, V., Plummer, D., Righi, M., Rumbold, S., Schulz, M., Skeie, R. B., Stevenson, D. S., Strode, S., Sudo, K., Szopa, S., Voulgarakis, A., and Zeng, G.: The Atmospheric Chemistry and Climate Model Intercomparison Project (ACCMIP): overview and description of models, simulations and climate diagnostics, *Geosci. Model Dev. Discuss.*, 5, 2445-2502, doi:10.5194/gmdd-5-2445-2012, 2012.

Lee, Y. H., Lamarque, J.-F., Flanner, M. G., Jiao, C., Shindell, D. T., Berntsen, T., Bisiaux, M. M., Cao, J., Collins, W. J., Curran, M., Edwards, R., Faluvegi, G., Ghan, S., Horowitz, L. W., McConnell, J. R., Myhre, G., Nagashima, T., Naik, V., Rumbold, S. T., Skeie, R. B., Sudo, K., Takemura, T., and Thevenon, F.: Evaluation of preindustrial to present-day black carbon and its albedo forcing from ACCMIP (Atmospheric Chemistry and Climate Model Intercomparison Project), *Atmos. Chem. Phys. Discuss*., 12, 21713-21778, doi:10.5194/acpd-12-21713-2012, 2012.

McConnell, J.R., and Edwards, R. Coal burning leaves toxic heavy metal legacy in the Arctic, *Proceedings of the National Academy of Sciences*, doi:10.1073/pnas.0803564105, 2008.

Moss, R. H., Edmonds, J. A., Hibbard, K. A., Manning, M. R., Rose, S. K., van Vuuren, D. P., Carter, T. R., Emori, S., Kainuma, M., Kram, T., Meehl, G. A., Mitchell, J. F. B., Nakicenovic, N., Riahi, K., Smith, S. J., Stouffer, R. J., Thomson, A. M.,Weyant, J. P., and Wilbanks, T. J. The next generation of scenarios for climate change research and assessment. *Nature,* 463, 747-756, doi:10.1038/nature08823, 2010.

Murphy, D. and Fahey, D., An estimate of the flux of stratospheric reactive nitrogen and ozone into the troposphere, *J. Geophys. Res*., 99, D3, 5325-5332, doi:10.1029/93JD03558, 1994.

Opel, T., Fritzche, D., Meyer, H., Schuett, R., Weiler, K., Ruth, U., Wilhelms, F. and Fischer, H. 115 year ice core record from Akademii Nauk ice cap, Servernaya Zemlya: high-resolution record of Euroasian Arctic climate change, *Journal of Glaciology,* 55(189), 21-31, 2009.

Phoenix, G. K., Hicks, W. K., Cinderby, S., Kuylenstierna, J. C. I., Stock, W. D., Dentener, F. J., Giller, K. E., Austin, A. T., Lefroy, R. D. B., Gimeno, B. S., Ashmore, M. R. and Ineson, P. Atmospheric Nitrogen Deposition in World Biodiversity Hotspots: the need for a greater global perspective in assessing N deposition impacts. *Global Change Biol.,* 12, 470–476, doi: 10.1111/j.1365-2486.2006.01104.x, 2006.

Prather, M. J., Holmes, C. D. and Hsu, J. Reactive greenhouse gas scenarios: Systematic exploration of uncertainties and the role of atmospheric chemistry, *Geophys. Res. Lett*., 39, L09803, doi:10.1029/2012GL051440, 2012.

Reay, D.S., Dentener, F., Smit, P., Grace, J. and Feely, R.A. Global nitrogen deposition and carbon sinks, *Nature Geoscience,* 1, 430 – 437, doi:10.1038/ngeo230, 2008.

Reichler, T. and Kim, J. How Well do Coupled Models Simulate Today's Climate? *Bull. Amer. Meteor. Soc,* 89, 303-311, 2008.

Rodhe, H., Dentener, F. and Schulz, M. The global distribution of acidifying wet deposition, *Environ. Science Tech*., 36, 4382-4388, 2002.

Roethlisberger, R., Bigler, M., Hutterli, M., Sommer, S., Stauffer, B., Junghans, H.G. and Wagenbach, D. Technique for continuous high-resolution analysis of trace substances in firn and ice cores, *Environ. Sci. Technol*., 34, 338–342, 606, 607, 2000.

Sanderson, M.G., Dentener, F.J., Fiore, A.M., Cuvelier, C., Keating, T.J., Zuber, A., Atherton, C.S., Bergmann, D.J., Diehl, T., Doherty, R.M., Duncan, B.N., Hess, P., Horowitz, L.W., Jacob, D., Jonson, J.-E., Kaminski, J.W., Lupu, A., Mackenzie, I.A., Marmer, E., Montanaro, V., Park, R., Pitari, G., Prather, M.J., Pringle, K.J., Schroeder, S., Schultz, M.G., Shindell, D.T., Szopa, S., Wild, O., and Wind, P.: A multi-model source-receptor study of the hemispheric transport and deposition of oxidised nitrogen, *Geophys. Res. Lett*., 35, L17815, doi:10.1029/2008GL035389, 2008.

Shindell, D. T., Lamarque, J.-F., Schulz, M., Flanner, M., Jiao, C., Chin, M., Young, P., Lee, Y. H., Rotstayn, L., Milly, G., Faluvegi, G., Balkanski, Y., Collins, W. J., Conley, A. J., Dalsoren, S., Easter, R., Ghan, S., Horowitz, L., Liu, X., Myhre, G., Nagashima, T., Naik, V., Rumbold, S., Skeie, R., Sudo, K., Szopa, S., Takemura, T., Voulgarakis, A., and Yoon, J.-H.: Radiative forcing in the ACCMIP historical and future climate

simulations, *Atmos. Chem. Phys. Discuss*., 12, 21105-21210, doi:10.5194/acpd-12-21105-2012, 2012.

Sigl, M., McConnell, J. R., Layman, L., Maselli, O., McGwire, K., Pasteris, D., Dahl-Jensen, D., Steffensen, J.P., Edwards, R. and Mulveney, R. A new bipolar ice core record of volcanism from WAIS Divide and NEEM and implications for climate forcing of the last 2000 years, *J. Geophys. Res*., doi:10.1029/2012JD018603, *In Press*, 2012.

Smith, S. J., van Aardenne, J., Klimont, Z., Andres, R. J., Volke, A., and Delgado Arias, S.: Anthropogenic sulfur dioxide emissions: 1850–2005, *Atmos. Chem. Phys*., 11, 1101-1116, doi:10.5194/acp-11-1101-2011, 2011.

Sutton, M. A., Oenema, O., Erisman, J. W., Leip, A., van Grinsven, H., and Winiwarter, W. Too much of a good thing, *Nature,* 472, 159-161, 2011.

Taylor, K. E., Stouff er, R. J., and Meehl, G. A.: An overview of CMIP5 and the experiment design, *B. Am. Meteorol. Soc*., 93, 485–498, 2012.
Thornton, P. E., Doney, S. C., Lindsay, K., Moore, J. K., Mahowald, N., Randerson, J. T., Fung, I., Lamarque, J.-F., Feddema, J. J. and Lee, Y.-H. Carbon-nitrogen interactions regulate climate-carbon cycle feedbacks: results from an atmosphere-ocean general circulation model. *Biogeosciences*, 6, 2099-2120, 2009.

van Aardenne, J.A., Dentener, F.J., Klijn Goldewijk, C.G.M., Lelieveld, J. and Olivier, J.G.J. A 1˚-1˚ resolution dataset of historical anthropogenic trace gas emissions for the period 1890-1990, *Global Biogeochem. Cy.,* 15, 909-928, 2001.

van Vuuren, D.P., Edmonds, J., Kainuma, M., Riahi, K., Thomson, A., Hibbard, K., Hurtt, G. C., Kram, T., Krey, V., Lamarque, J.-F., Matsui, T., Meinshausen, M., Nakicenovic, N., Smith, S. J. and Rose, S. K. The Representative Concentration Pathways: An overview. *Climatic Change*, 109, 5-31, DOI: 10.1007/s10584-011-0148-z, 2011.

Vet R., Artz, R., Shaw, M., Ro, C-U, Carou, S., Aas, W., Baker, A., Bowersox, V., Dentener, F., Galy-Lacaux, C., Pienaar, K., Gillett, R., Forti, M.C., Gromov S., Hara, H., Khodzher, T., Mahowald, N., Nickovic, N., Rao, P.S.P., and Reid, N. A Global Assessment of Precipitation Chemistry and Deposition. In preparation. 2013.

Wolff, E., Ice sheets and nitrogen, Accepted for publication in the *Philosophical Transactions of the Royal Society, Series B*, 2013.

Xie, P., and Arkin, P.A. Global precipitation: A 17-year monthly analysis based on gauge observations, satellite estimates, and numerical model outputs. *Bull. Amer. Meteor. Soc.,* 78, 2539 – 2558, 1997.

Xing, J., Pleim, J., Mathur, R., Pouliot, G., Hogrefe, C., Gan, C.-M., and Wei, C.: Historical gaseous and primary aerosol emissions in the United States from 1990–2010,

Atmos. Chem. Phys. Discuss., 12, 30327-30369, doi:10.5194/acpd-12-30327-2012, 2012.

Yang, D., Kane, D., Zhang, Z., Legates D., and Goodison, B. Bias-corrections of long-term (1973-2004) daily precipitation data over the northern regions, *Geophys. Res. Lett*., 32, L19501, doi:10.1029/2005GL024057, 2005.

Young, P. J., Archibald, A. T., Bowman, K. W., Lamarque, J.-F., Naik, V., Stevenson, D. S., Tilmes, S., Voulgarakis, A., Wild, O., Bergmann, D., Cameron-Smith, P., Cionni, I., Collins, W. J., Dalsøren, S. B., Doherty, R. M., Eyring, V., Faluvegi, G., Horowitz, L. W., Josse, B., Lee, Y. H., MacKenzie, I. A., Nagashima, T., Plummer, D. A., Righi, M., Rumbold, S. T., Skeie, R. B., Shindell, D. T., Strode, S. A., Sudo, K., Szopa, S., and Zeng, G.: Pre-industrial to end 21st century projections of tropospheric ozone from the Atmospheric Chemistry and Climate Model Intercomparison Project (ACCMIP), *Atmos. Chem. Phys. Discuss*., 12, 21615-21677, doi:10.5194/acpd-12-21615-2012, 2012.

Zaehle, S., Friedlingstein, P. and Friend, A. D. Terrestrial nitrogen feedbacks may accelerate future climate change, *Geophys. Res. Lett*., 37, doi: 10.1029/2009GL041345, 2010.

Zhang, L., Jacob, D. J., Knipping, E. M., Kumar, N., Munger, J. W., Carouge, C. C., van Donkelaar, A., Wang, Y. X., and Chen, D.: Nitrogen deposition to the United States: distribution, sources, and processes, *Atmos. Chem. Phys*., 12, 4539-4554, doi:10.5194/acp-12-4539-2012, 2012.

Historical simulations	**1850**	**1930**	**1980**	**2000**
Emissions and SSTs/GHGs for given year	P	P	P	P
Future simulations	**2010**	**2030**	**2050**	**2100**
RCP 2.6 (emissions, GHGs and SSTs)		P	O	P
RCP 4.5 (emissions, GHGs and SSTs)	O	O	O	O
RCP 6.0 (emissions, GHGs and SSTs)	P	P	O	P
RCP 8.5 (emissions, GHGs and SSTs)		P	O	P

Table 1. List and principal characteristics of ACCMIP simulations (P indicates the primary simulations, O the optional ones). SSTs stands for sea-surface temperatures and GHGs for greenhouse gases. Adapted from Lamarque et al. (2013).

Model	Dry	Wet	Total dep.	eminox	emilnox	Total emi.
					Tg(N)/yr	
CESM-CAM-superfast	17	29	46	42	4	46
CMAM	27	23	50	47	4	51
GEOSCCM	12	33	45	40	5	45
GISS-E2-R	14	39	53	41	8	49
GISS-E2-TOMAS	17	37	54	41	8	49
MOCAGE	20	27	47	43	5	48
NCAR-CAM3.5	20	29	49	43	4	47
STOC-HadAM3	26	27	52	45	7	52
UM-CAM	31	26	56	49	5	54
Multi-model mean	20	30	50	47	6	49
PhotoComp			51			

Table 2. Summary of global totals (Tg(N)/year) for deposition and emissions in 2000 related to the nitrogen oxide emissions. Total dep. (4th column) is the sum of wet and dry deposition while Total emi. (6th column) is the sum of NOx surface and aircraft emissions (eminox) and lightning emissions (emilnox). Note that deposition is slightly larger than emissions due to the net input of nitrogen (usually in the form of nitric acid) from the stratosphere (approx. 1 Tg(N)/year, except for the GISS models which have a 5 Tg(N)/year input from the stratosphere).

Model	Dry NH_3	Wet NH_3	Dry NH_4	Wet NH_4	Total	eminh3
	Tg(N)/year					
GISS-E2-R	22	5	4	29	58	57
NCAR-CAM3.5	14	16	7	24	60	59
STOC-HadAM3	29	8	6	19	61	62
Multi-model mean	19	9	5	25	60	60
PhotoComp					64	

Table 3. Summary of global totals (Tg(N)/year) for year 2000 of deposition and emissions related to the ammonia emissions. Total (6^{th} column) is the sum of wet and dry deposition for NH_3 and NH_4. Eminh3 includes anthropogenic and natural (soils and oceans) emissions.

Model	Dry	Wet	Total dep.	emiso2	emiso4	emidms	Total emi.
	Tg(S)/year						
CESM-CAM-superfast	36	45	81	64	0	19	83
GISS-E2-R	51	45	95	65	2	28	95
NCAR-CAM3.5	24	55	79	64	0	19	83
NCAR-CAM5.1	25	56	81	65	1	18	84
STOC-HadAM3	41	43	84	69	0	20	89
Multi-model mean	33	50	83	64	1	20	84
PhotoComp			80				

Table 4. Summary of global totals (Tg(S)/year) for year 2000 of deposition and emissions related to the sulfur emissions. Total dep. (4th column) is the sum of wet and dry deposition (both sums of SO_2 and SO_4) while Total emi. (8th column) is the sum of SO_2, SO_4 and DMS emissions. Note that the deposition total should be smaller than emission total since the formation of sulfate from the oxidation of DMS has a yield smaller than 1; this was estimated to be 87% in Boucher et al. (2003) when both gas-phase and aqueous-phase reactions are taken into account.

	wetno3								
	North America			Europe			Asia		
	PhotoComp	HTAP	ACCMIP	PhotoComp	HTAP	ACCMIP	PhotoComp	HTAP	ACCMIP
Linear fit slope	1.0	1.0	0.9	0.3	0.3	0.3	0.5	0.5	0.4
Linear fit intercept	-15.4	-10.3	-18.7	16.0	25.0	33.2	22.2	23.1	21.3
Mean bias	-0.4	-0.2	-0.5	0.4	0.6	0.7	0.4	0.5	0.4
Mean observations	1.9	1.9	1.9	3.0	3.0	3.0	2.6	2.6	2.6
Mean model	2.3	2.1	2.4	2.6	2.4	2.3	2.2	2.1	2.2
Correlation coefficient	0.8	0.9	0.9	0.6	0.6	0.6	0.8	0.8	0.8
Fraction within +/-50%	77.0	84.3	68.3	75.0	85.2	85.2	84.0	84.0	88.0

	wetnh4								
	North America			Europe			Asia		
	PhotoComp	HTAP	ACCMIP	PhotoComp	HTAP	ACCMIP	PhotoComp	HTAP	ACCMIP
Linear fit slope	0.8	0.9	0.4	0.4	0.4	0.3	0.8	0.7	0.1
Linear fit intercept	-3.3	-6.3	17.1	7.7	17.3	46.3	21.1	18.8	77.9
Mean bias	-0.1	-0.1	0.2	0.3	0.5	0.9	0.7	0.6	1.7
Mean observations	1.6	1.6	1.6	3.4	3.4	3.4	4.0	4.0	4.0
Mean model	1.7	1.7	1.4	3.1	2.9	2.3	3.3	3.4	2.3
Correlation coefficient	0.9	0.9	0.8	0.6	0.6	0.6	0.8	0.8	0.2
Fraction within +/-50%	82.2	84.8	73.0	73.9	79.5	76.1	76.0	68.0	48.0

	wetso4								
	North America			Europe			Asia		
	PhotoComp	HTAP	ACCMIP	PhotoComp	HTAP	ACCMIP	PhotoComp	HTAP	ACCMIP
Linear fit slope	0.9	1.0	0.7	0.4	0.6	0.3	0.4	0.5	0.4
Linear fit intercept	-13.0	-13.9	-2.4	19.9	-11.3	32.7	46.8	36.1	61.7
Mean bias	-0.5	-0.5	-0.1	0.6	-0.6	1.0	2.2	1.9	2.7
Mean observations	3.1	3.1	3.1	4.0	4.0	4.0	6.9	6.9	6.9
Mean model	3.6	3.6	3.2	3.4	4.6	3.0	4.7	5.0	4.2
Correlation coefficient	0.9	0.9	0.9	0.6	0.6	0.7	0.9	0.9	0.9
Fraction within +/-50%	70.4	70.0	68.3	78.7	52.8	82.0	80.0	88.0	72.0

Table 5. Summary of statistical analysis of the evaluation of nitrate wet deposition (wetno3), ammonium wet deposition (wetnh4) and sulfate wet deposition (wetso4) for PhotoComp, HTAP and ACCMIP MMM over the 3 main analysis regions.

	United States			Europe		
Model	wetnoy	eminox	precip	wetnoy	eminox	precip
CESM-CAM-superfast	4.8	0.6	4.2	-1.4	-14.2	0.5
CMAM	7.3	3.8	-1.7	-12.7	-9.2	1.9
GEOSCCM	2.4	1.2	-0.6	-15.5	-13.6	0.3
GISS-E2-R	-0.8	-2.4	-0.3	-14.2	-11.3	2.9
GISS-E2-TOMAS	6.2	1.6	-0.3	-9.6	-10.8	2.9
MOCAGE	4.8	1.6	1.8	-3.1	-11.1	-3.3
NCAR-CAM3.5	6.5	1.6	2.4	-12.1	-13.2	0.8
STOC-HadAM3	9.9	1.8	2.6	-4.7	-10.6	4.1
UM-CAM	2.7	-2.0	-0.2	-4.9	-13.2	4.1
Multi-model mean	4.9	0.9	0.9	-8.7	-11.9	1.6

Table 6. Relative change 2000 *minus* 1980 (expressed in %, relative to 1980) for NO_y wet deposition (wetnoy), NOx emissions (eminox) and total precipitation averaged over the region of interest.

Region	2000	RCP26 2100	RCP45 2100	RCP85 2100
Canada	203	150	148	201
USA	619	416	412	550
Mexico	423	464	351	503
C. America	260	313	242	287
Brazil	334	397	299	465
Rest of S. America	255	369	253	359
N. Africa	180	139	132	211
W. Africa	384	524	450	573
E. Africa	291	461	355	570
S. Africa	295	389	258	458
W. Europe	776	448	467	662
C. Europe	1054	685	577	1256
Turkey	697	541	512	657
Ukraine	852	584	415	1049
Kazakhstan area	294	361	201	328
Russia	287	205	188	304
Middle East	267	278	190	383
South Asia	740	1550	1023	1318
Korea region	1025	921	751	894
East Asia	778	1021	690	888
Southeast Asia	624	827	569	752
Indonesia	679	694	297	417
Japan	736	447	447	660
Oceania	130	133	118	153
Greenland	54	39	46	58

Table 7. Average nitrogen (NHx+NOy) deposition (mg(N)/m^2/year) over specific regions as defined in Lamarque et al. (2011). Filled boxes indicate regions where the deposition increase with respect to 2000.

Region	2000	RCP26 2100	RCP45 2100	RCP85 2100
Canada	160	38	34	45
USA	502	65	71	75
Mexico	423	76	121	93
C. America	264	119	165	119
Brazil	119	52	67	69
Rest of S. America	168	90	116	112
N. Africa	132	48	96	67
W. Africa	127	103	115	126
E. Africa	122	73	89	97
S. Africa	151	148	79	133
W. Europe	527	98	141	107
C. Europe	1073	127	188	146
Turkey	737	136	205	130
Ukraine	797	80	129	98
Kazakhstan area	256	39	61	99
Russia	195	40	46	60
Middle East	300	54	73	155
South Asia	435	74	155	289
Korea region	1271	209	242	277
East Asia	694	71	93	108
Southeast Asia	394	132	162	182
Indonesia	372	292	270	249
Japan	886	414	515	431
Oceania	111	56	81	64
Greenland	37	21	18	25

Table 8. Average sulfur deposition (mg(S)/m^2/year) over specific regions as defined in Lamarque et al. (2011). The deposition does not increase in any of these regions with respect to 2000.

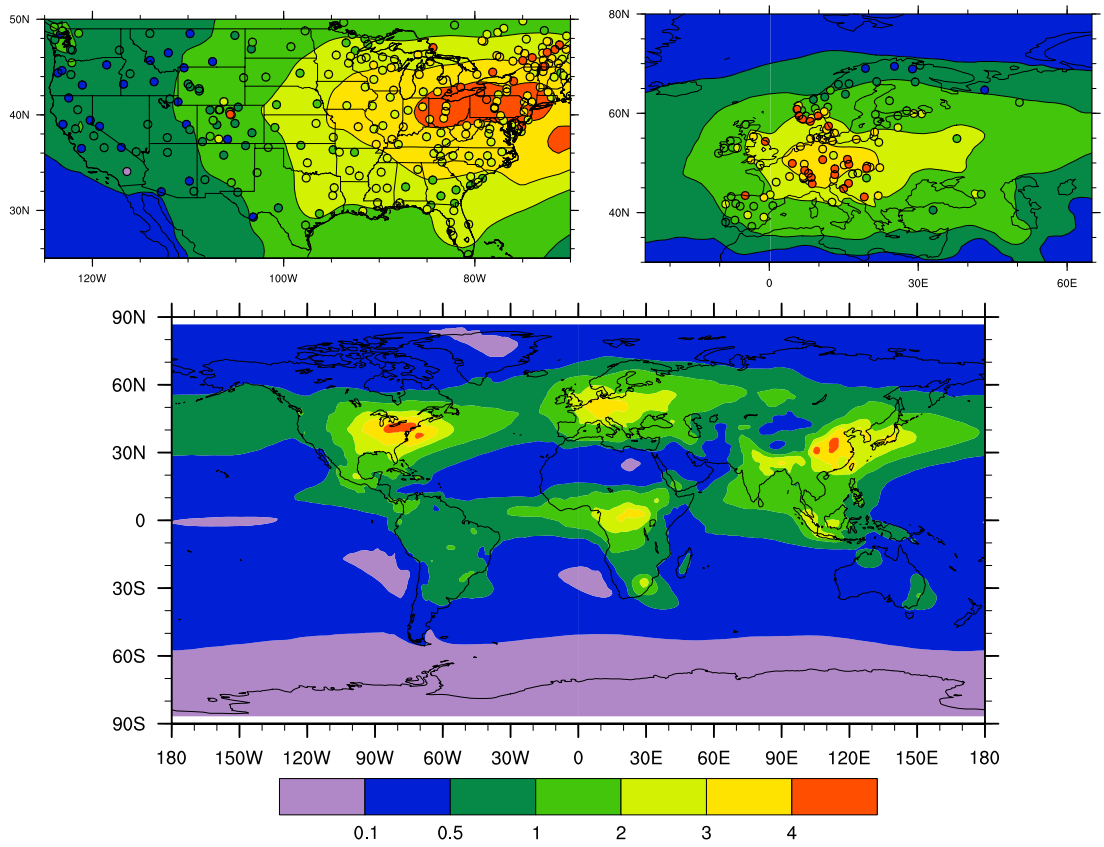

Figure 1a. Nitrate wet deposition (kg(N)/ha/year) for 2000. Contours are for the multi-model mean, filled circles are for the wet deposition network observations.

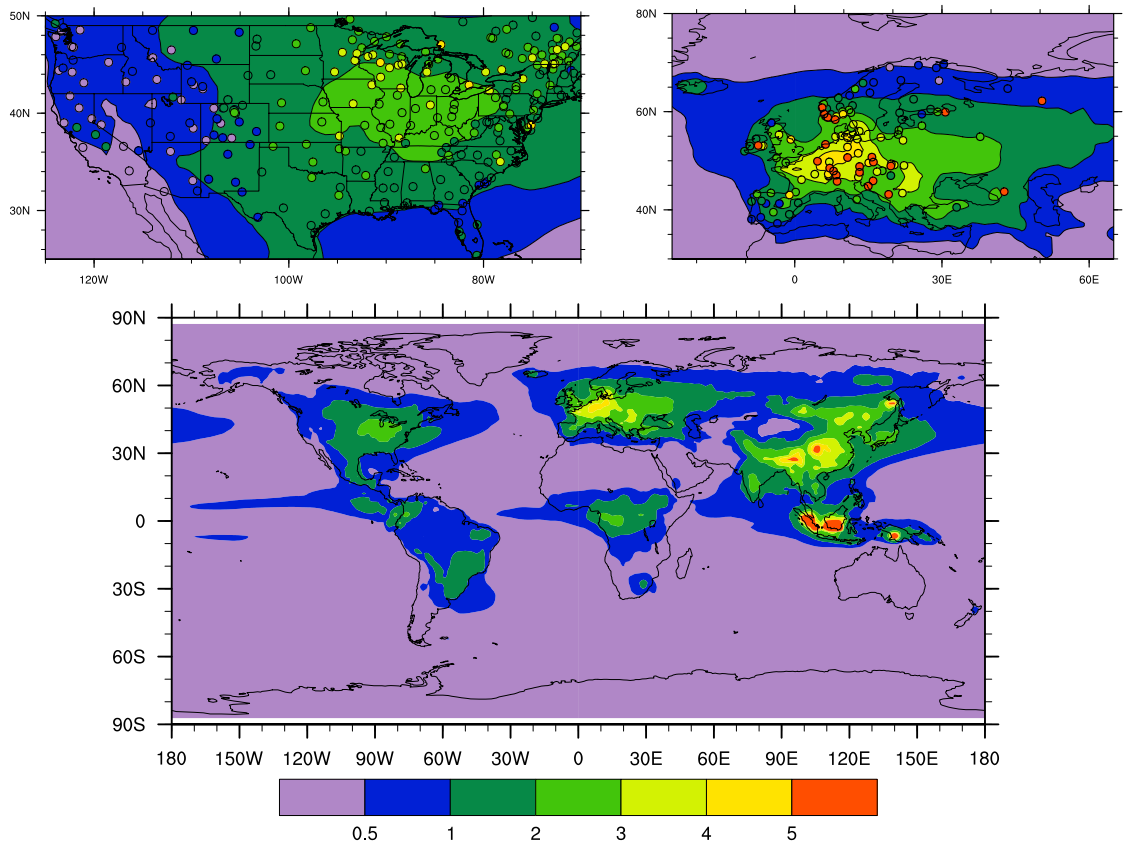

Figure 1b. Ammonium wet deposition (kg(N)/ha/year) for 2000. Contours are for the multi-model mean, filled circles are for the wet deposition network observations.

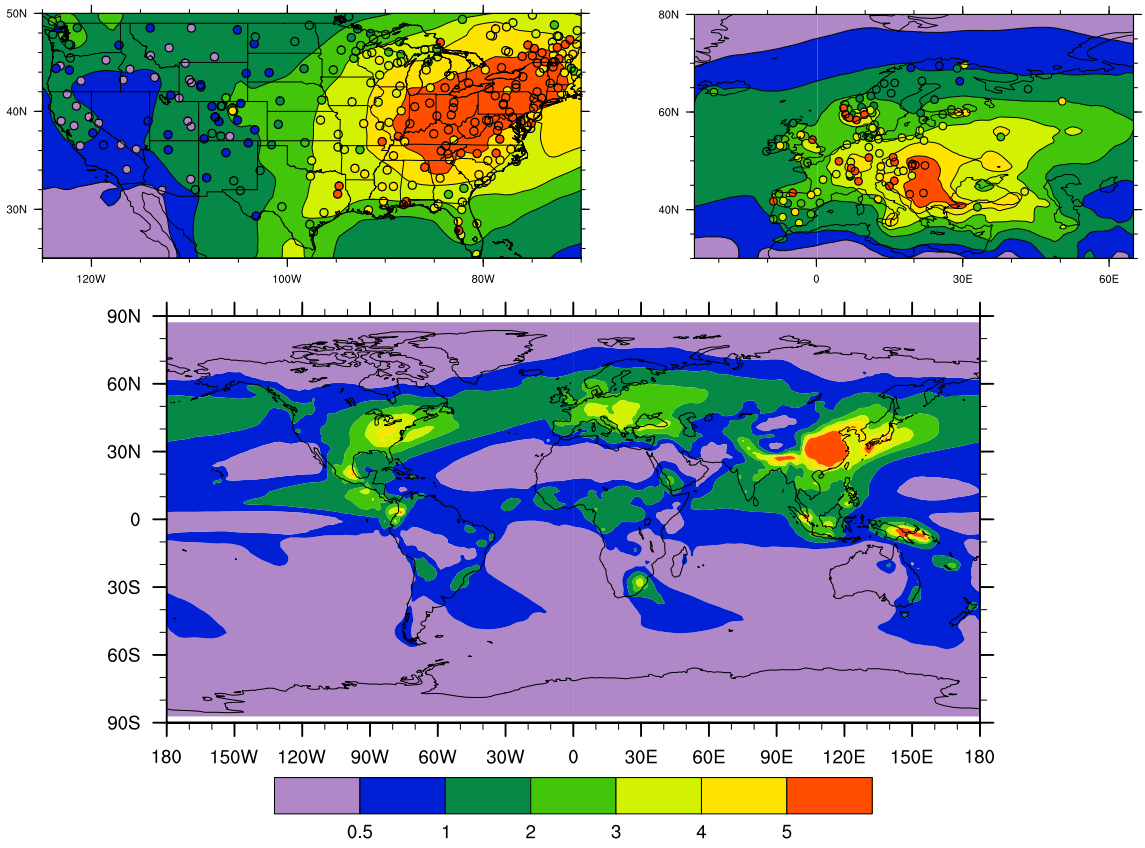

Figure 1c. Sulfate wet deposition (kg(S)/ha/year) for 2000. Contours are for the multi-model mean, filled circles are for the wet deposition network observations.

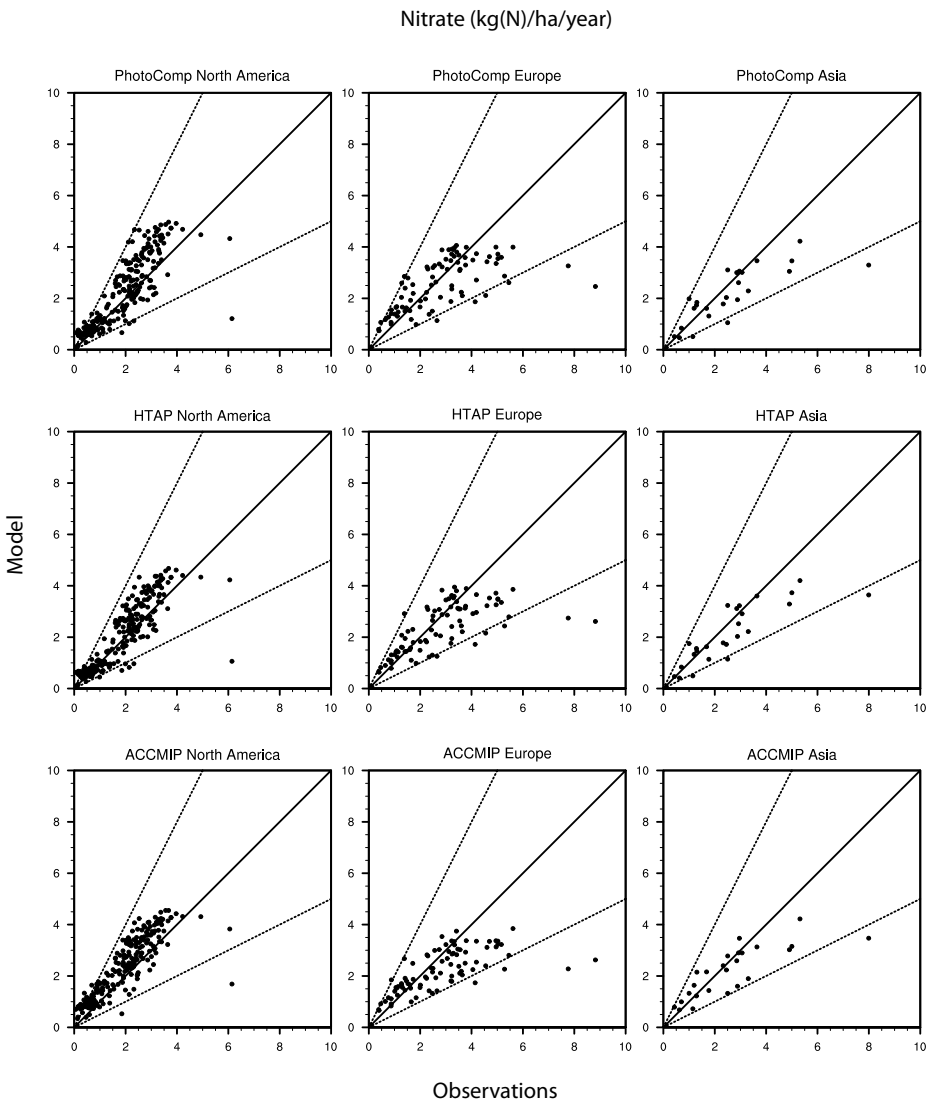

Figure 2a. Scatterplot of nitrate wet deposition (kg(N)/ha/yr) over North America (left column), Europe (middle column) and East Asia (right column). Top row shows the model results from PhotoComp, middle row from HTAP and bottom row from this study. See text for details.

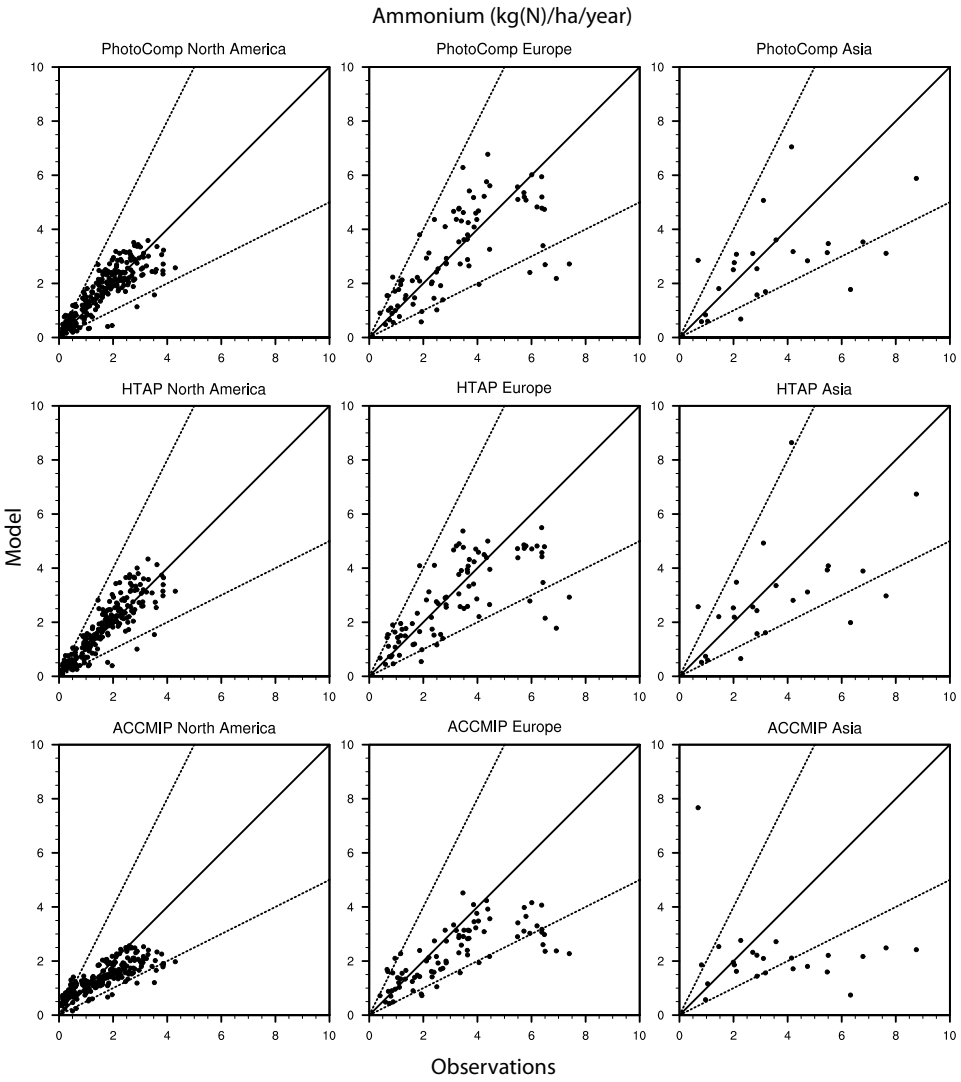

Figure 2b. Scatterplot of ammonium wet deposition (kg(N)/ha/yr) over North America (left column), Europe (middle column) and East Asia (right column). Top row shows the model results from PhotoComp, middle row from HTAP and bottom row from this study. See text for details.

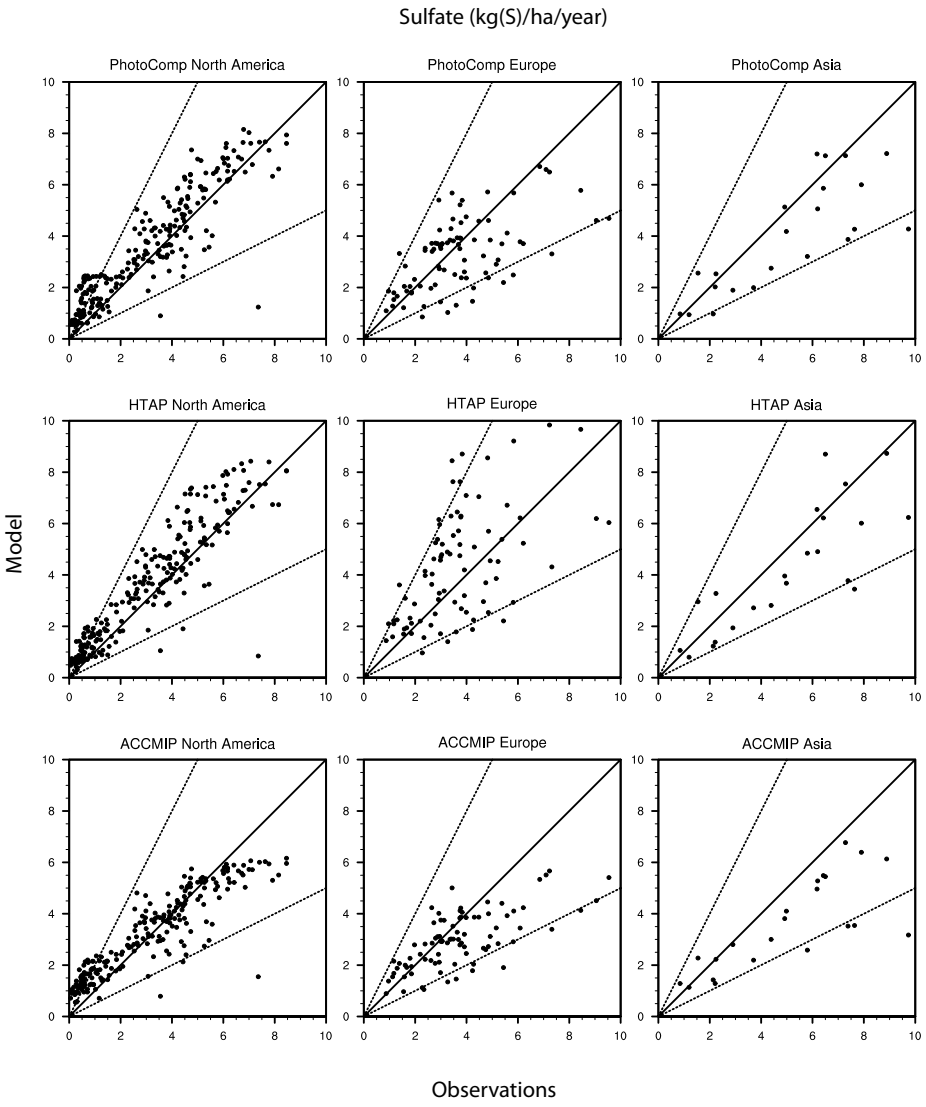

Figure 2c. Scatterplot of sulfate wet deposition (kg(S)/ha/yr) over North America (left column), Europe (middle column) and East Asia (right column). Top row shows the model results from PhotoComp, middle row from HTAP and bottom row from this study. See text for details.

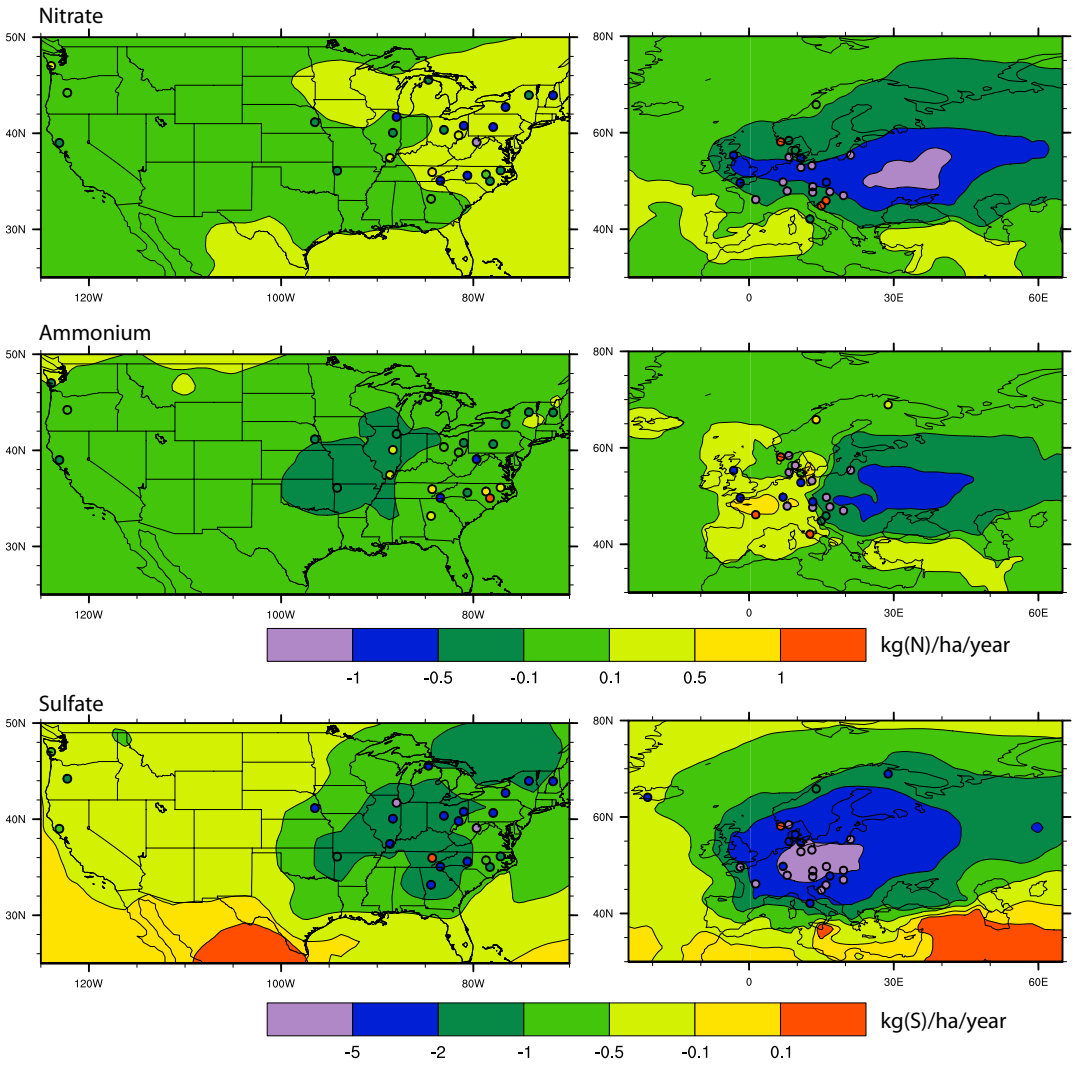

Figure 3. Change in deposition (2000-1980) over the NADP (left column) and EMEP (right column) networks. Top row is for nitrate (kg(N)/ha/year), middle row is for ammonium (kg(N)/ha/year), bottom row is for sulfate (Kg(S)/ha/year).

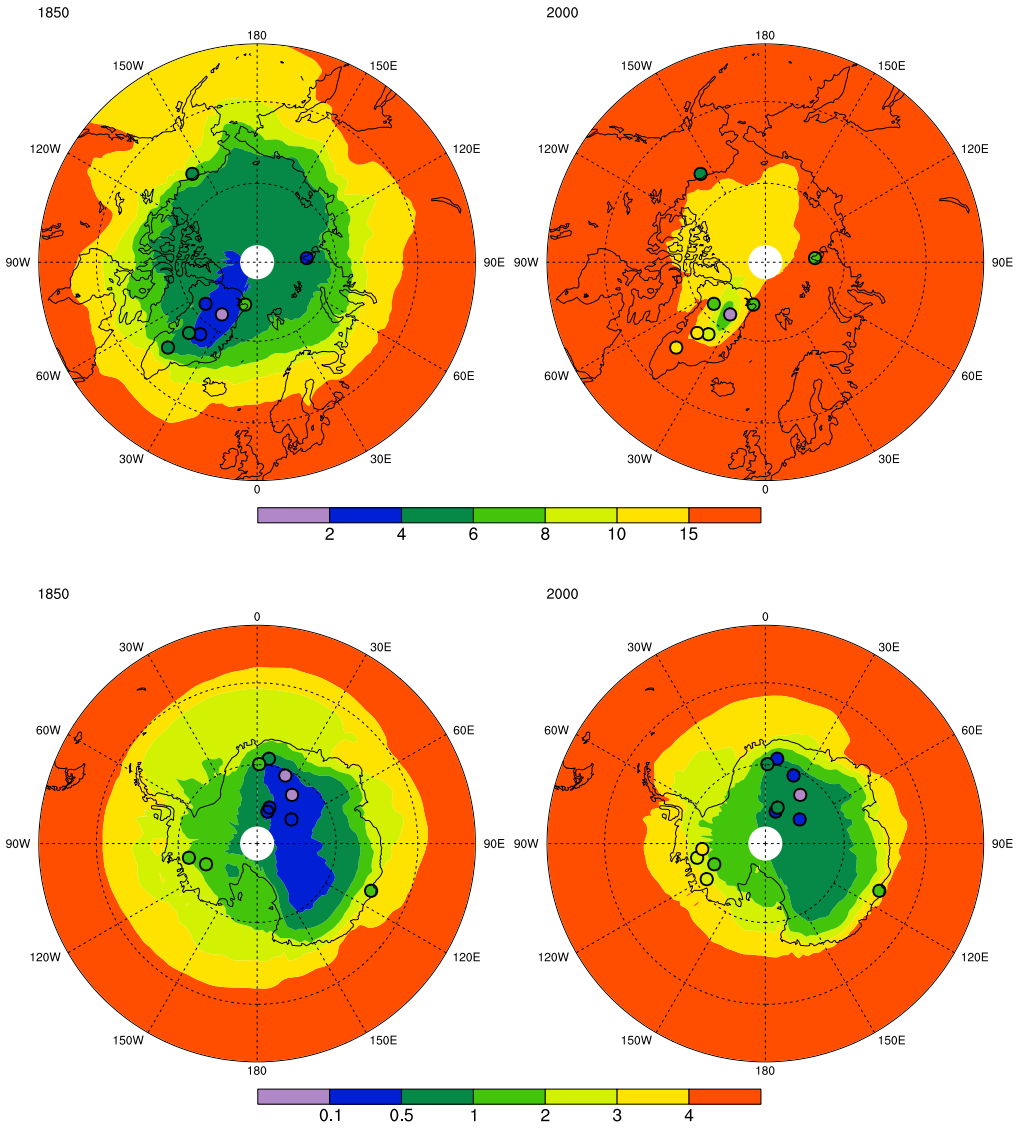

Figure 4a. Nitrate deposition from ice-cores (mg(N)/m2/year, filled circles, see Table S5) and MMM for 1850 (left column) and 2000 (right column). Note different color scales.

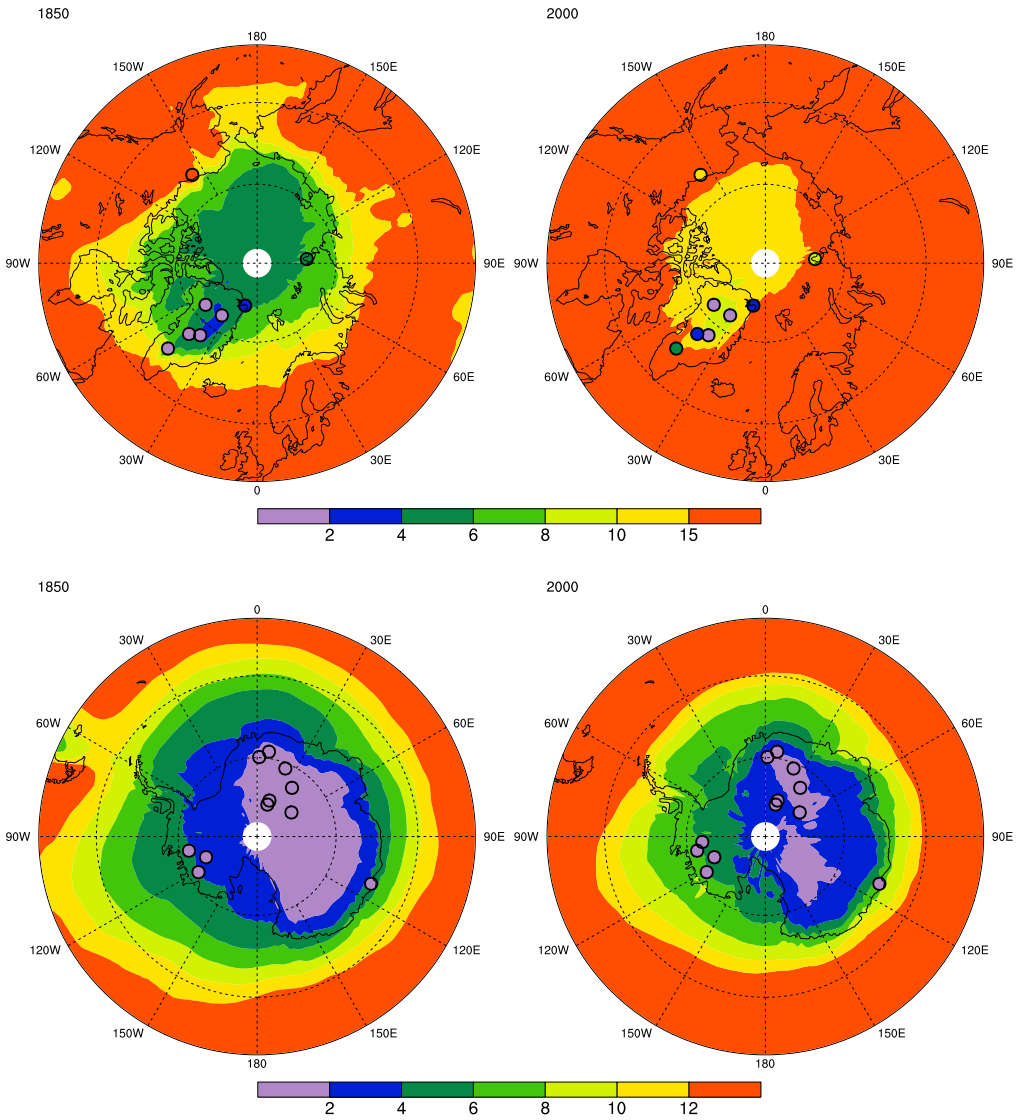

Figure 4b. Ammonium deposition from ice-cores (mg(N)/m2/year, filled circles, see Table S5) and MMM for 1850 (left column) and 2000 (right column). Note different color scales.

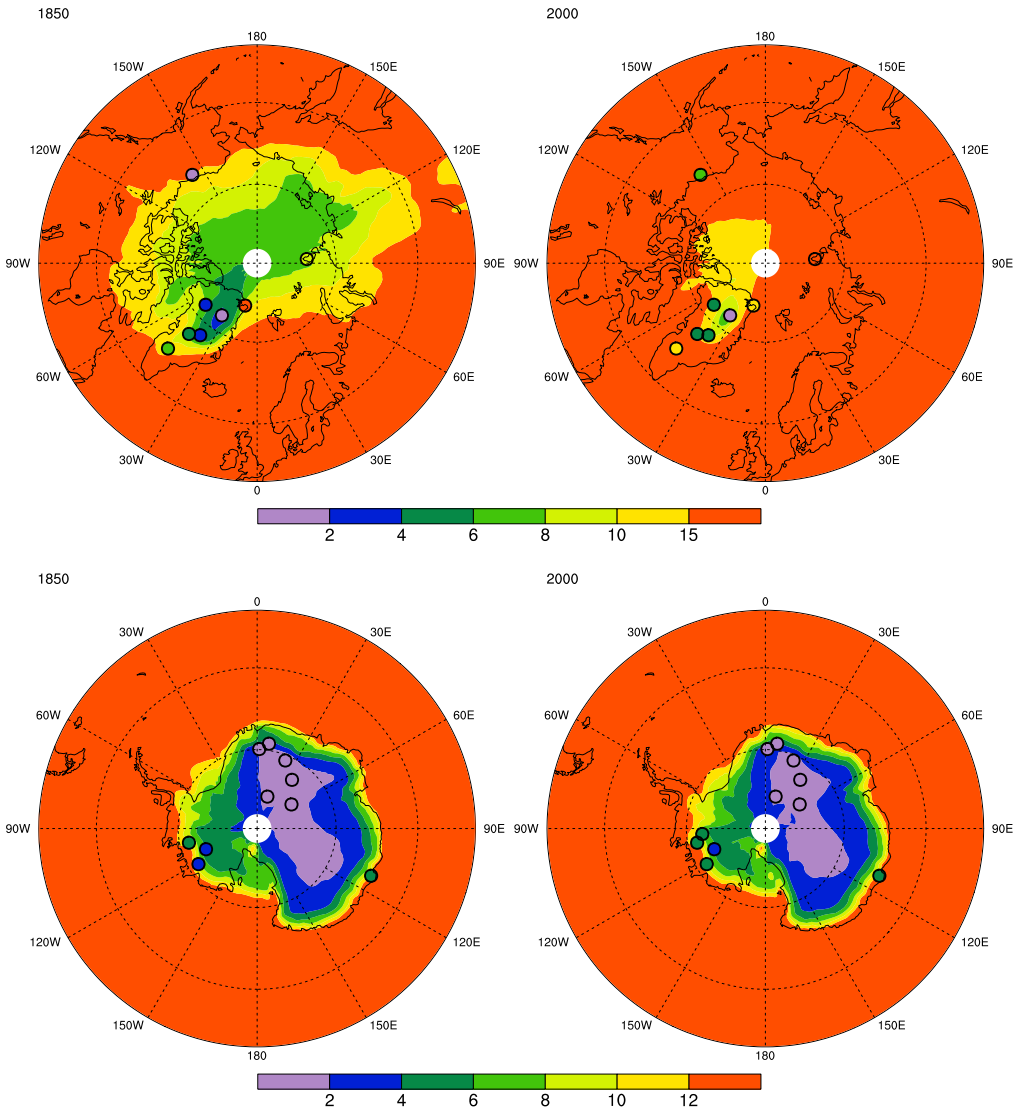

Figure 4c. Sulfate deposition from ice-cores (mg(S)/m2/year, filled circles, see Table S5) and MMM for 1850 (left column) and 2000 (right column). Note different color scales.

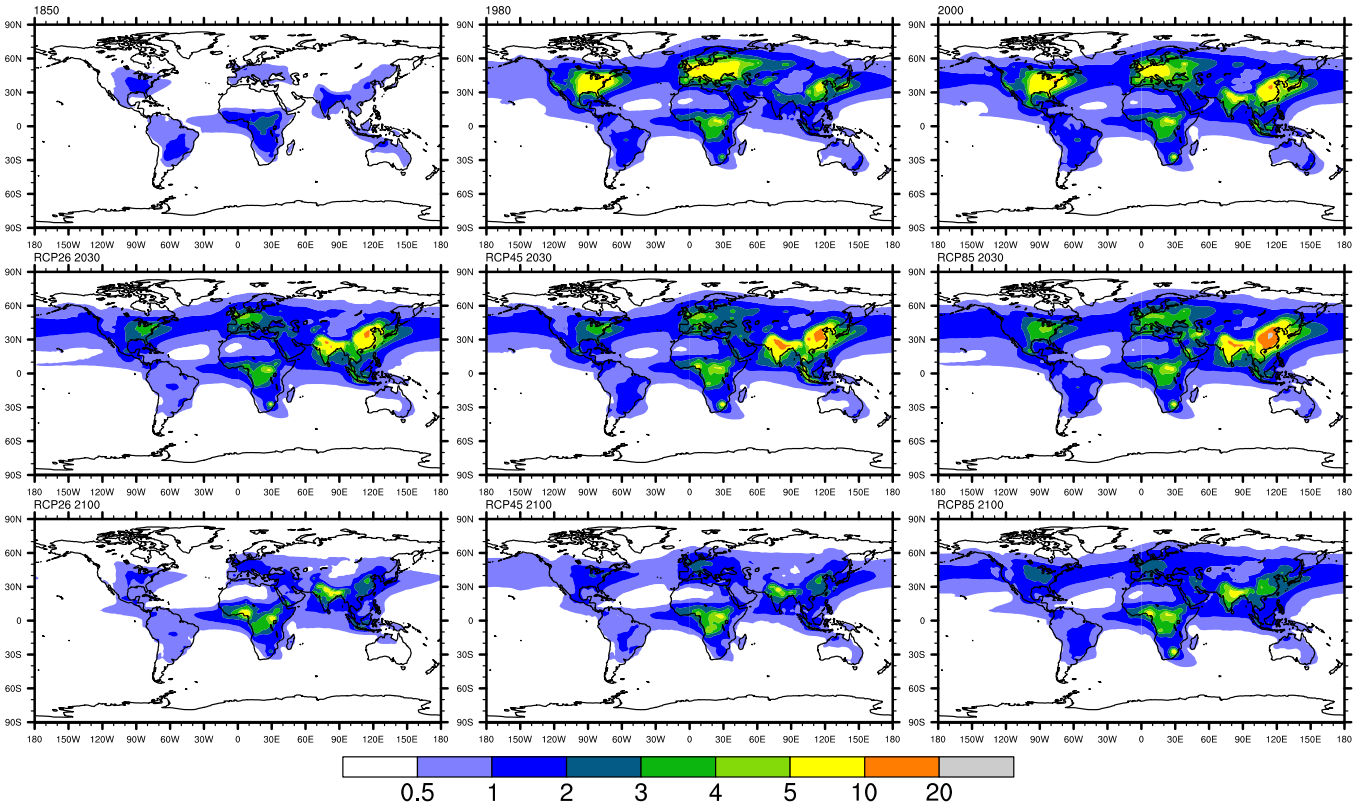

Figure 5a. Total (wet + dry) NOy deposition 1850-2100 (kg(N)/ha/year).

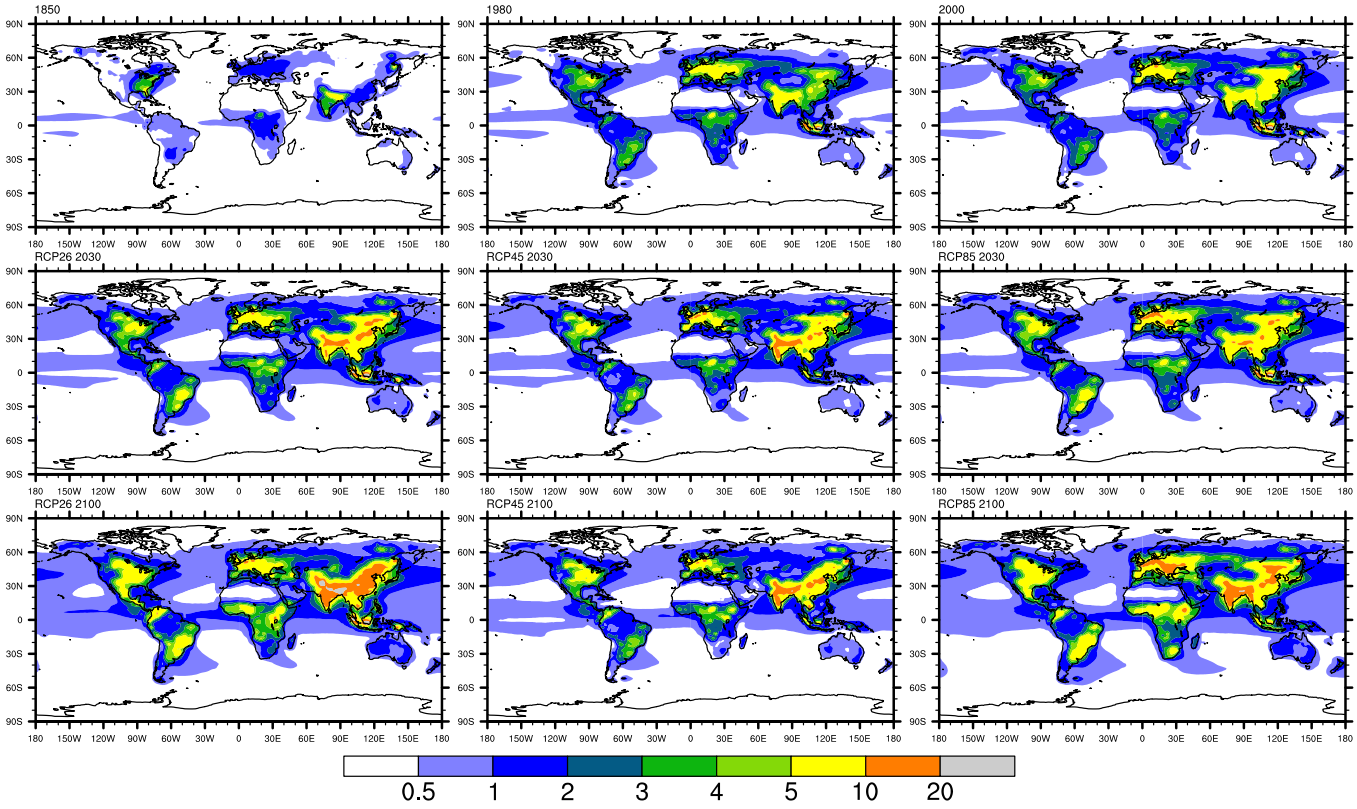

Figure 5b. Total (wet + dry) NHx deposition 1850-2100 (kg(N)/ha/year).

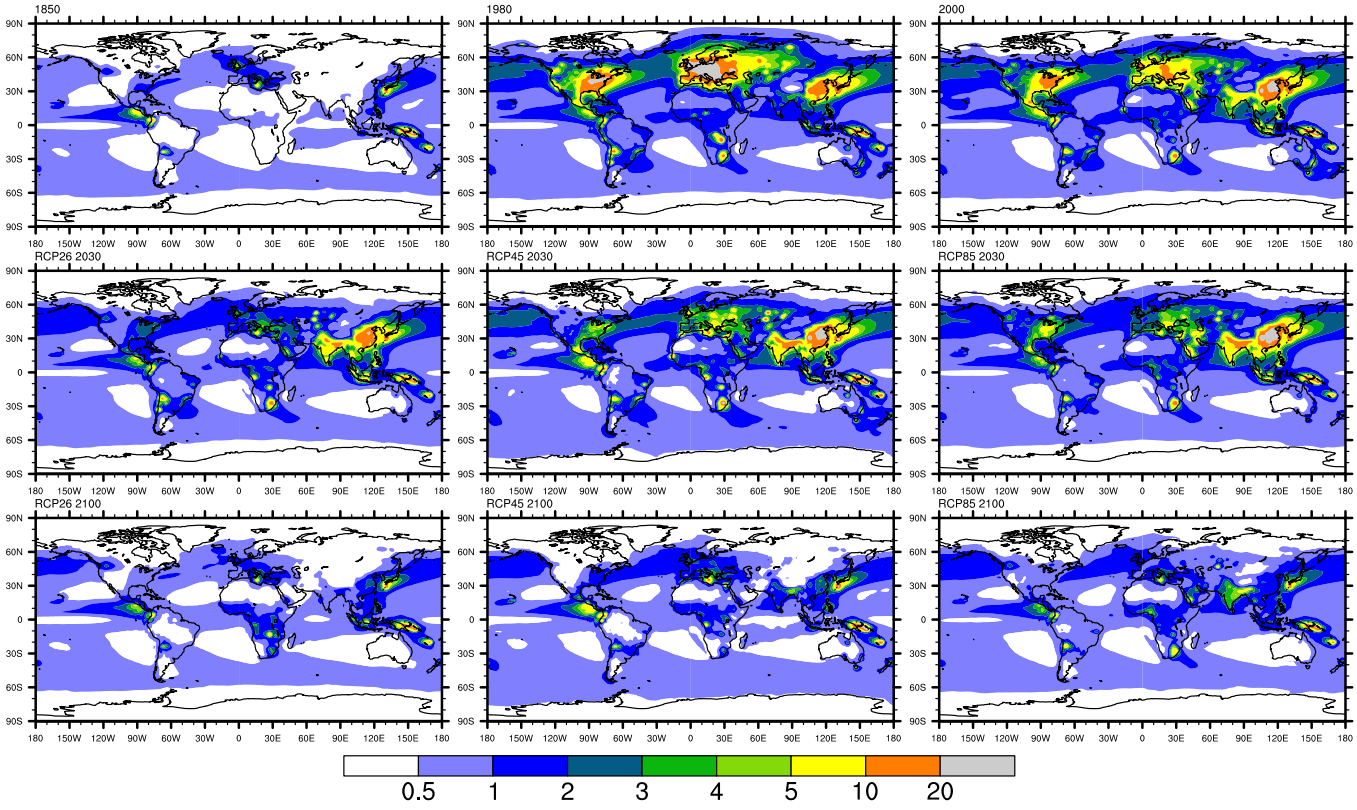

Figure 5c. Total (wet + dry) SOx deposition 1850-2100 (kg(S)/ha/year).

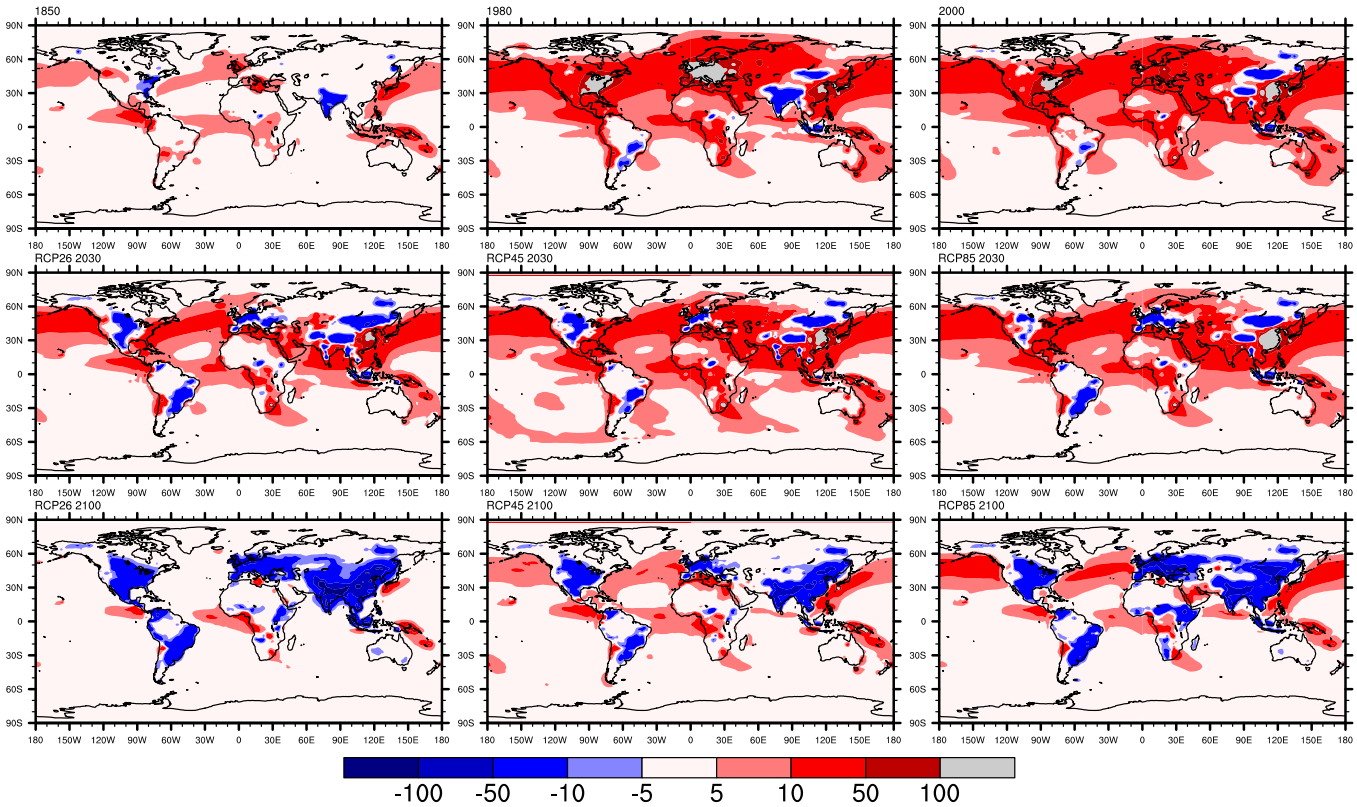

Figure 6. Time evolution of deposition acidity (10^{-6} moles/m^2/year) computed as $2*SO_x + NO_y - NH_x$. Blue regions indicate areas where deposition is more basic than it would have been without those respective emissions.